Multiwavelength Studies of Blazar Sources

Lukasz Stawarz
ルカシュ　スタヴァージュ

ISAS/JAXA, Japan
Jagiellonian University, Poland

Outline of the Talk

- **Introduction**

- Active Galactic Nuclei (AGN)
- Relativistic Jets in AGN
- Blazar Phenomenon

- **Open Questions**

- Flat Spectrum Radio Quasars (FSRQs)
- BL Lacertae Objects (BL Lacs)
- "Misaligned" Blazars (Radio Galaxies)

- **Conclusions**

Active Galactic Nuclei

Each galaxy hosts supermassive (M_{BH} ~ 10^6 - 10^{10} $M_\odot$) black hole in its center, and each supermassive black hole accretes at some level from the surrounding interstellar medium. Active Galactic Nuclei (AGN) are associated with those supremassive black holes which accrete at higher rates.

AGN constitute a very diverse class of astrophysical sources. They differ in the properties of their large-scale environments, in the properties of their host galaxies, in the accretion rates and accretion fuels, in the structure and state of their circumnuclear environment, in the masses (and spins?) of central black holes, and finally in the physical parameters of the produced outflows.

- Quasars (~ 10^{-7} Mpc^{-3})
  - Radio-quiet or radio-loud quasars
- BL Lacertae Objects (~ 10^{-7} Mpc^{-3})
- Radio Galaxies (~ 10^{-6} Mpc^{-3})
  - Broad or narrow line radio galaxies
  - Fanaroff-Riley class I or II
  - …and many more…
- Seyfert Galaxies (~ 10^{-4} Mpc^{-3})
  - Seyferts type 1 - 2
  - Narrow-Line Seyferts
- Low-Luminosity AGN (> 10^{-3} Mpc^{-3})
  - LINERs
  - Sgr A* (?)

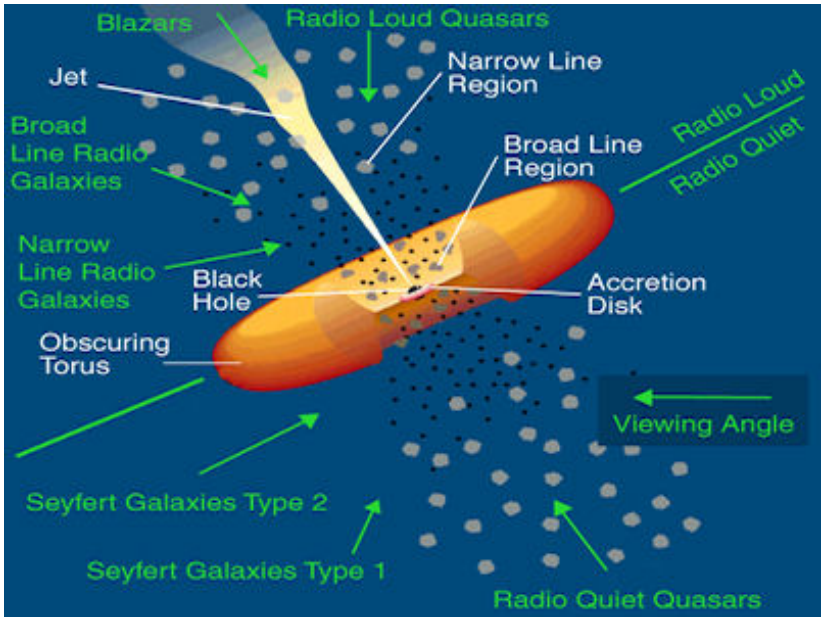

Urry & Padovani 95

Relativistic Jets

For a rotating black hole embedded in an external magnetic field (supported by an accretion disk) power can be extracted by allowing currents to flow between the equator and poles of a spinning black hole above the event horizon.

Blandford & Znajek 1977 discussed how, with a force-free magnetosphere added to such a rotating black hole, electromagnetic currents are driven an the energy is released (in a form of magnetized jets) in the expense of the black hole rotational energy ("reducible mass"). This scenario was inspired by earlier developed models for young stars (Weber & Davis 1967), pulsars (Michel 1969, Goldreich & Julian 1970), and accretion disks in active galaxies (Blandford 1976, Lovelace 1976, Bisnovatyi-Kogan & Ruzmaikin 1976), and is being recently investigated further by means of GR MHD simulations (e.g., Koide et al. 2002, Komissarov 2005, McKinney & Gammie 2004).

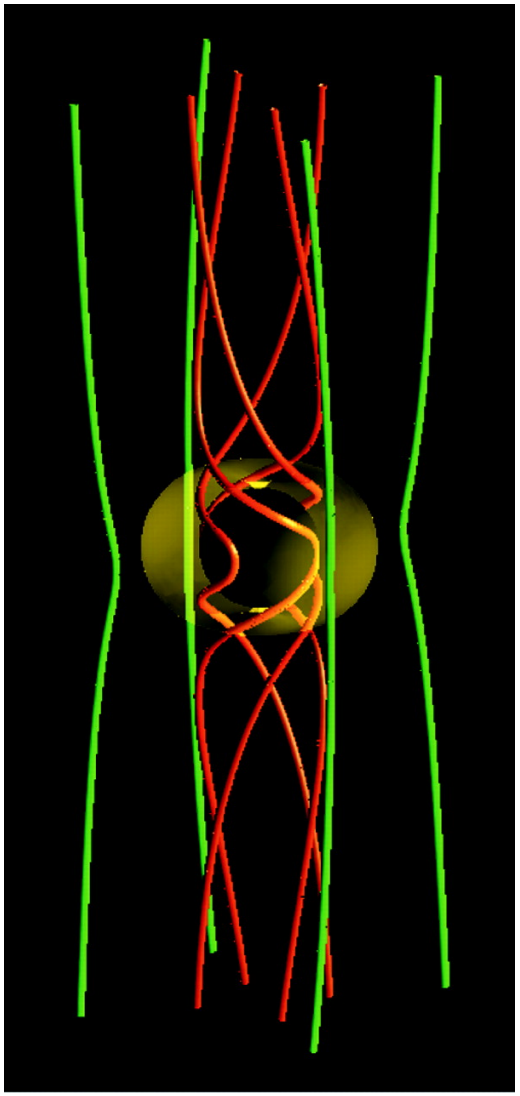

$$R_g = GM_{BH}/c^2 \sim 10^{14}\,(M_{BH}/10^9 M_\odot)\ \mathrm{cm}$$
$$L_{Edd} = 4\pi G M_{BH} m_p c/\sigma_T \sim 10^{47}\,(M_{BH}/10^9 M_\odot)\ \mathrm{erg/s}$$

for a maximally spinning ($J = J_{max}$) black hole:

$$E_{tot} \sim 0.3\, M_{BH}c^2 \sim 10^{63}\,(M_{BH}/10^9 M_\odot)\ \mathrm{erg}$$
$$P_{max} \sim cB^2R_g^{\,2}/4\pi \sim 10^{46}\,(M_{BH}/10^9 M_\odot)\ \mathrm{erg/s}$$

Blazars

Blazar sources: radio-loud AGN, for which the radiative output is dominated by a broad-band, variable and non-thermal emission of the innermost parts of relativistic jets.
Radio jets of blazars on mas scales show typically superluminal motions up to $\beta_{app} \approx 30$.
Rather heterogeneous blazar family includes luminous Flat Spectrum Radio Quasars (FSRQs) and low-power BL Lacertae Objects (Bl Lacs).

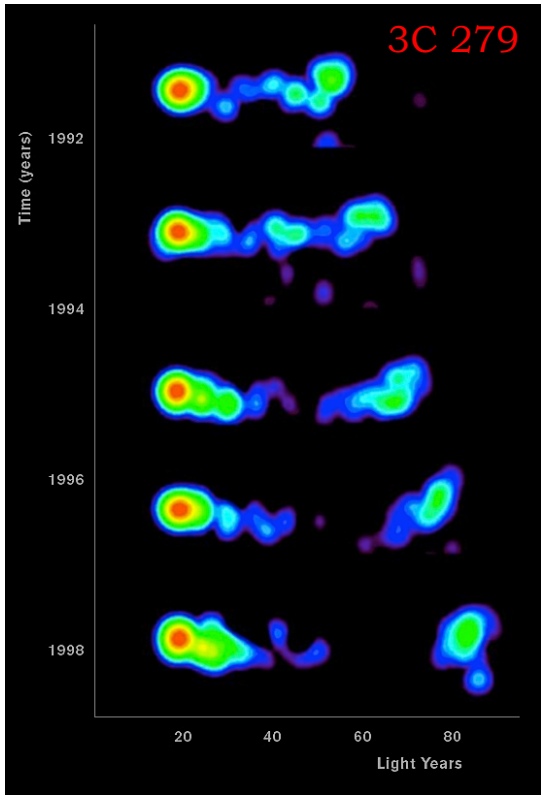

Blazar emission zone is unresolved even for radio interferometers.

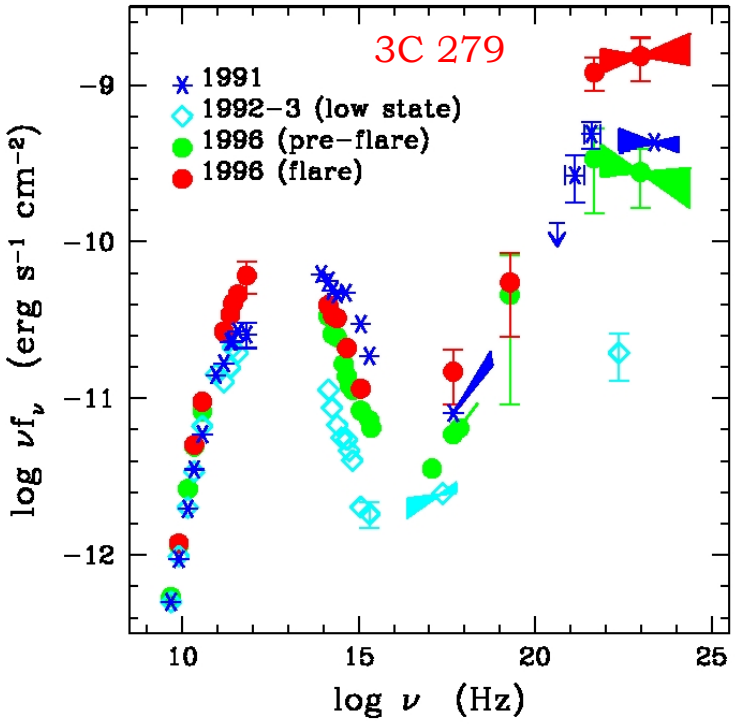

Multiwavelength studies are crucial for understanding blazar sources.

“Standard” Blazar Model

In the framework of the “standard” modeling of blazar sources, single homogeneous emission zone located at the distances of about 10^2-10^3 R_g ~ 10^{16}-10^{17} cm was assumed. This zone was typically associated with a jet region where strong shocks forms due to collisions of different portions of the jet plasma ejected with different bulk velocities from the core. Particle acceleration was proposed to be due to 1st-order Fermi process taking place at such shocks.

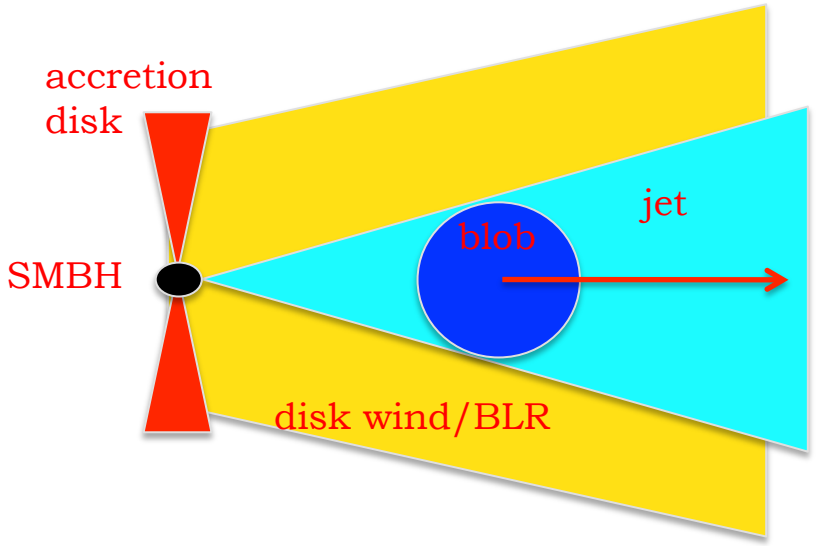

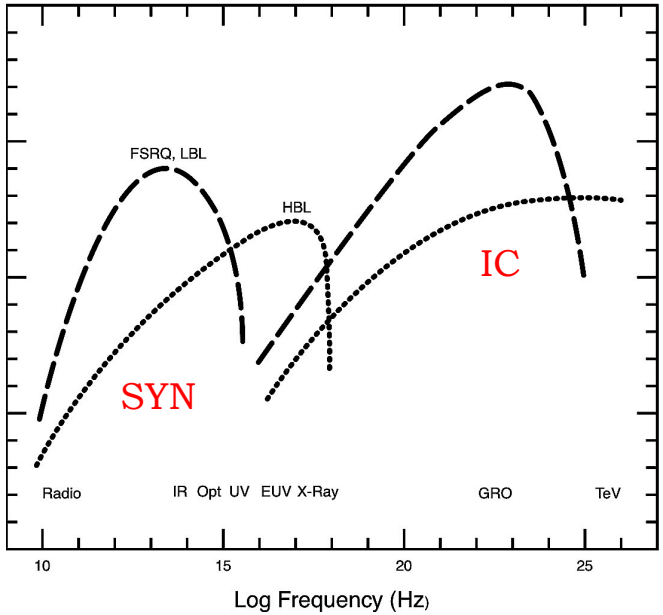

Leptonic Models (Maraschi et al. 91, Dermer & Schlickeiser 93, Sikora et al. 94, Levinson & Blandford 95, Marscher & Travis 96): Low- and high energy components due to synchrotron and inverse-Compton emission of ultrarelativistic electrons accelerated directly within the outflow.

Hadronic Models (Mannheim & Biermann 92, Mannheim 93): High-energy emission of relativistic protons directly accelerated within the outflow (photomezon production, synchrotron proton emission); low-energy component due to synchrotron emission of primary or secondary electrons.

Ultrarelativistic Particles

Strongly magnetized jets produced by spinning SMBHs are believed to be quickly accelerated and collimated to reach terminal bulk velocities of the order of $\Gamma_j \sim 10 - 30$ at sub-pc/pc distances from the jet base. At such distances, where the jet Poynting flux is expected to be at least partially converted to the bulk kinetic energy of the jet particles, shocks may form due to various reasons (e.g., kink instabilities, reconfinement by the ambient medium), and jet particles may be accelerated to ultrarelativistic energies ($e^{\pm}$ up to at least 10 TeV). Fermi acceleration at relativistic magnetized shocks is however hardly understood (see, e.g., Begelman & Kirk 90, Hoshino et al. 92, Bednarz & Ostrowski 98, Sironi & Spitkovsky 09).

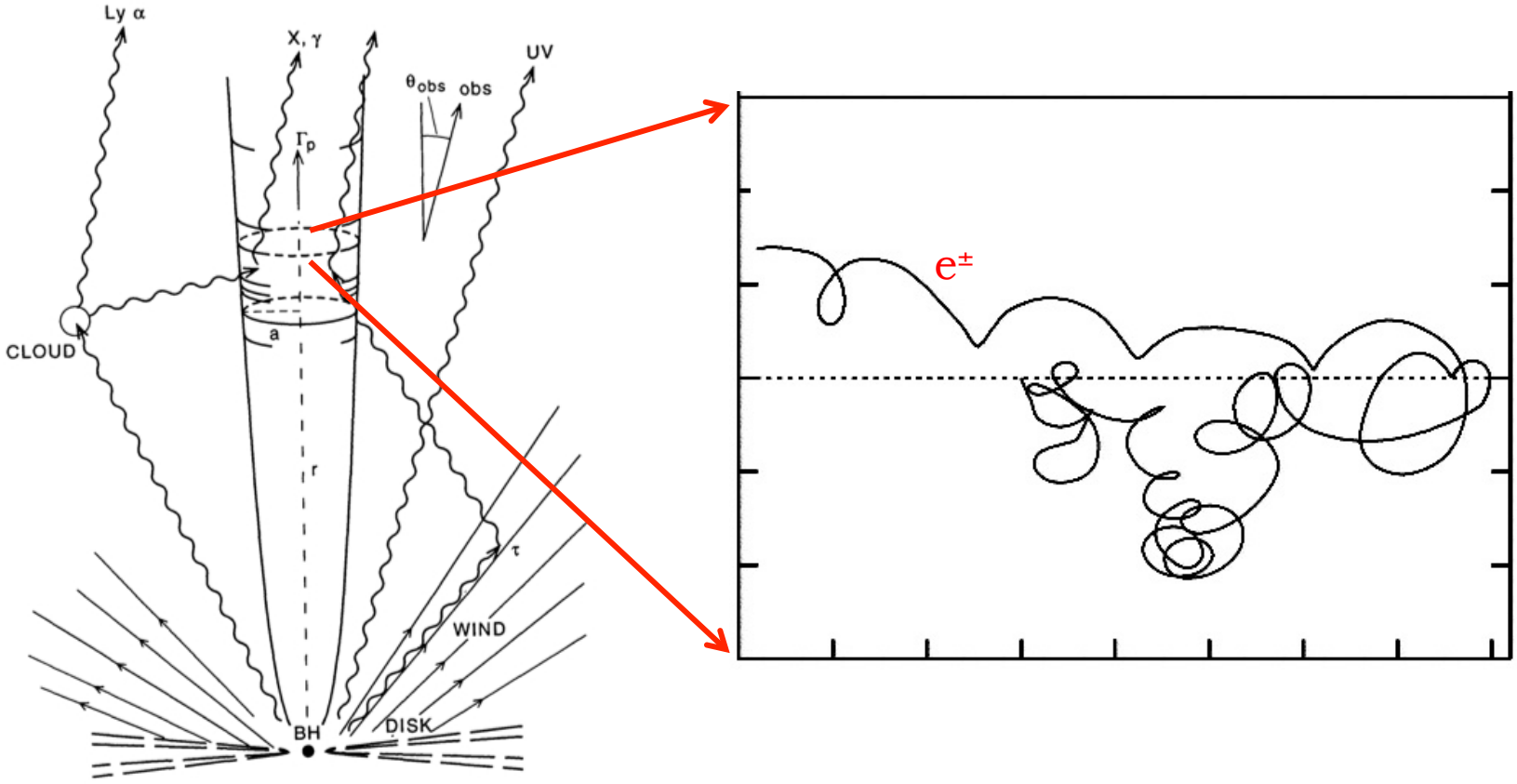

Nonthermal Emission

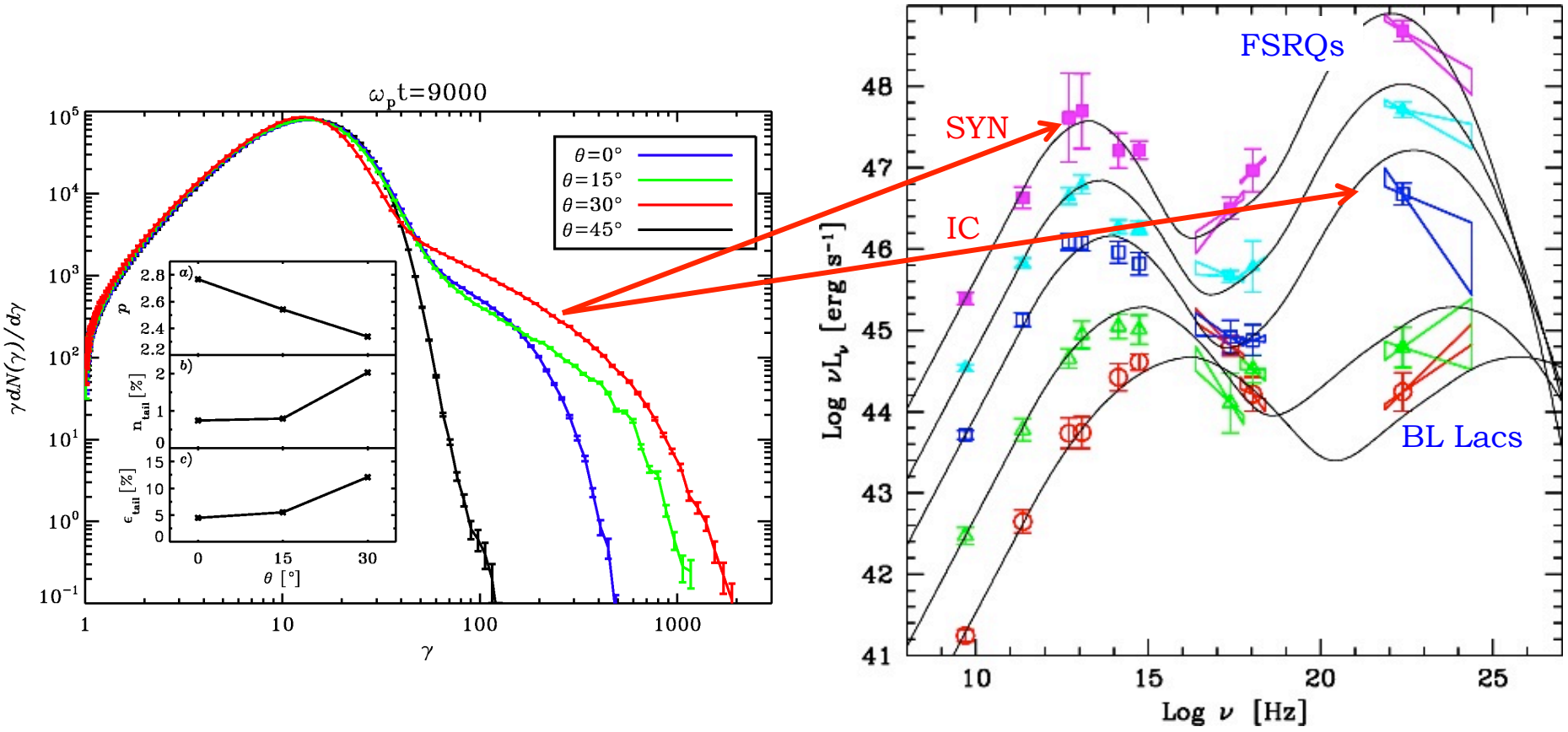

Non-thermal broad-band emission of the accelerated particles is Doppler-boosted in the observed rest frame, if a relativistic jet is viewed at angles $\theta \leq 1/\Gamma_j$ this results in the observed luminosities $L_{obs} = \delta^4 L'$ reaching 10^{44}-10^{49} erg/s ("blazar sources"; $\delta = \Gamma_j^{-1} [1 - \beta_j \cos\theta]^{-1}$ is the Doppler factor).

As demonstrated by the previous observations with the EGRET instrument onboard Compton Gamma-Ray Observatory, most of the jet power in luminous blazars is radiated in gamma-rays.

Open Questions

Studying blazar sources across the electromagnetic spectrum will not help us to answer all the open questions regarding AGN and relativistic jets. But at least some of the pressing issues can be addressed.

- **Internal structure of relativistic jets**
  Is there really only one, homogeneous and compact region of the enhanced energy dissipation within the outflow, rather than a superposition of different emission zones? If so, where exactly is the blazar emission zone?

- **Jet content and energetics**
  Are extragalactic jets purely leptonic, or do they contain also hadrons? Are hadrons important only for the global jet energetic, or do they also play a role in shaping radiative properties of AGN jets? Are AGN jets Poynting-flux dominated only in their innermost parts, or also at larger distances from the jet base? Is the jet composition changing substantially with the distance from the center?

- **Particle acceleration processes**
  Is the 1st order Fermi acceleration the dominant process in accelerating jet particles to ultrarelativistic energies, or are the other processes (turbulent acceleration, magnetic reconnection) equally/more relevant? Are the particle acceleration processes in relativistic regime substantially different than in non-relativistic regime?

Luminous FSRQs

Energy distribution of the radiating electrons in luminous FSRQs is always of a broken power-law form with the low-energy slope p<2 and high-energy slope q>2 (not a cooling break!)

e.g., Kataoka et al. 08 for PKS 1510-089

$$n_e(\gamma) \propto \begin{cases} \gamma^{-p} & \text{for} \quad \gamma < \gamma_{\rm br} \\ \gamma^{-q} & \text{for} \quad \gamma > \gamma_{\rm br} \end{cases}$$

Parameter	Model A
minimum electron Lorentz factor $\gamma_{\rm min}$	1
break electron Lorentz factor $\gamma_{\rm br}$	100
maximum electron Lorentz factor $\gamma_{\rm max}$	10^5
low-energy electron spectral index p	1.35
high-energy electron spectral index q	3.25
normalization of the injection function K_e	$0.9 \times 10^{47}\,{\rm s}^{-1}$
bulk Lorentz factor of the emitting plasma $\Gamma_{\rm jet}$	20
jet opening angle $\theta_{\rm jet}$	0.05 rad
jet viewing angle $\theta_{\rm obs}$	0.05 rad
scale of the emission zone $r_{\rm sh}$	10^{18} cm
jet magnetic field intensity B	1.3 G
scale of the dominant external photon field $r_{\rm ext}$	3.0×10^{18} cm
luminosity of the external photon field $L_{\rm ext}$	$3.7 \times 10^{45}\,{\rm erg\,s}^{-1}$
photon energy of the external photon field $h\nu_{\rm ext}$	0.2 eV
total energy of radiating electrons E_e	1.3×10^{48} erg
comoving electron energy density u'_e	$0.015\,{\rm erg\,cm}^{-3}$
equipartition magnetic field $B_{\rm eq}$	0.6 G
kinetic luminosity of radiating electrons L_e	$1.4 \times 10^{45}\,{\rm erg\,s}^{-1}$
soft X-ray excess	bulk-Compton

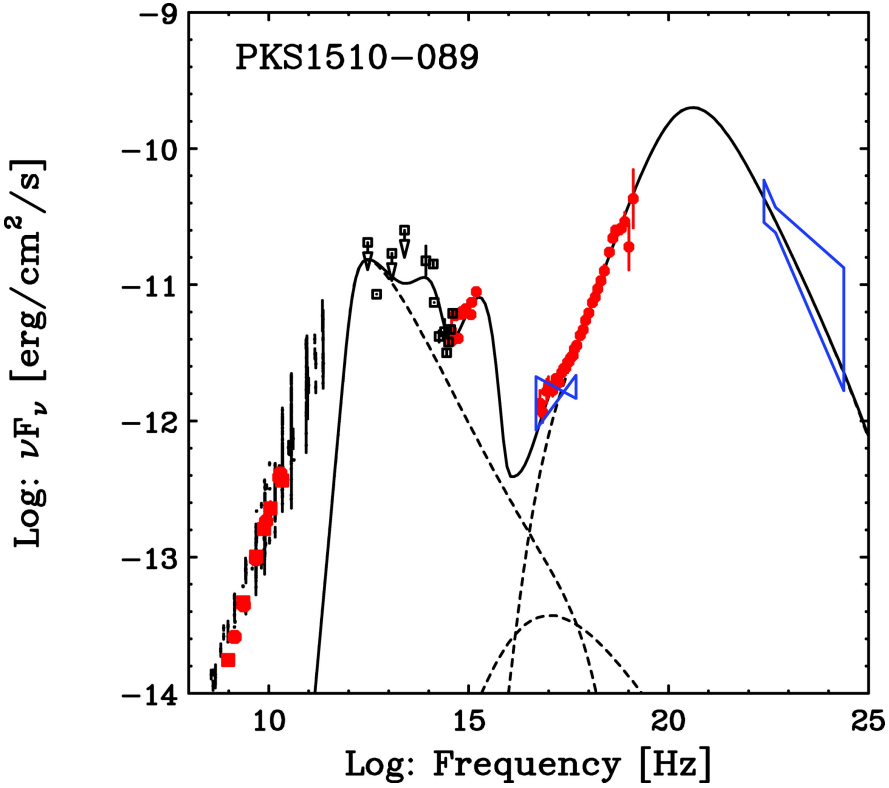

Modeling of the broad-band SED of luminous FSRQs typically indicate that the jet magnetic field at the position of the blazar emission zone is not relevant dynamically. On the other hand, bulk kinetic energy of the radiating electrons seems also not enough to account for the whole power carried by the outflow.

Heavy Jets

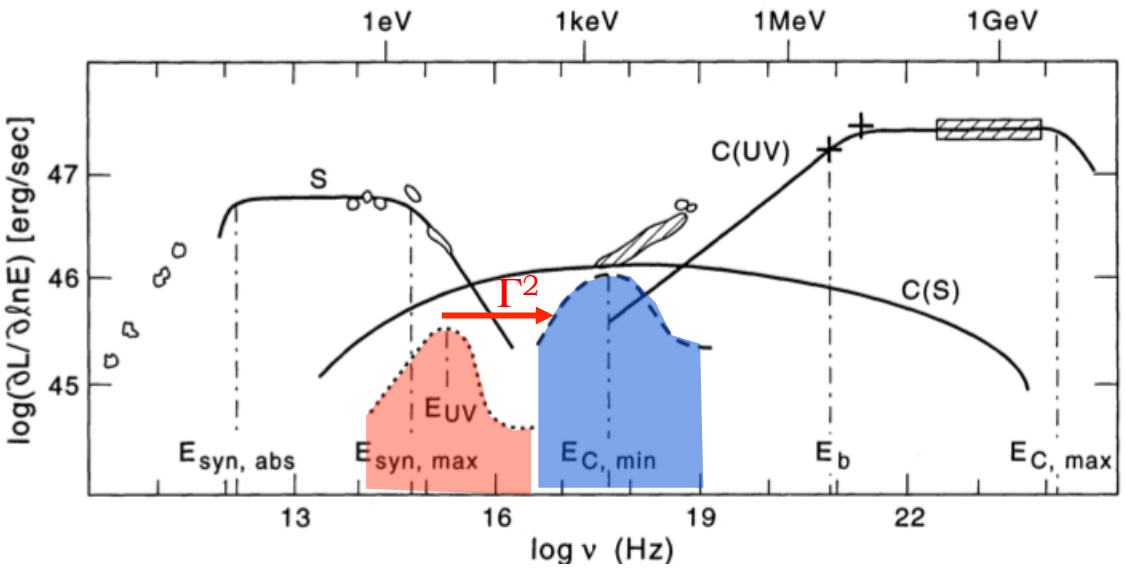

Lack of bulk-Compton features in soft-X-ray spectra of blazars indicates that there are not enough cold electrons to carry bulk of the jet kinetic power. This indicates a dynamical role of (cold) protons (Begelman & Sikora 87, Sikora et al. 97, Sikora & Madejski 00, Moderski et al. 04, Celotti et al. 07, Celotti & Ghisellini 08)

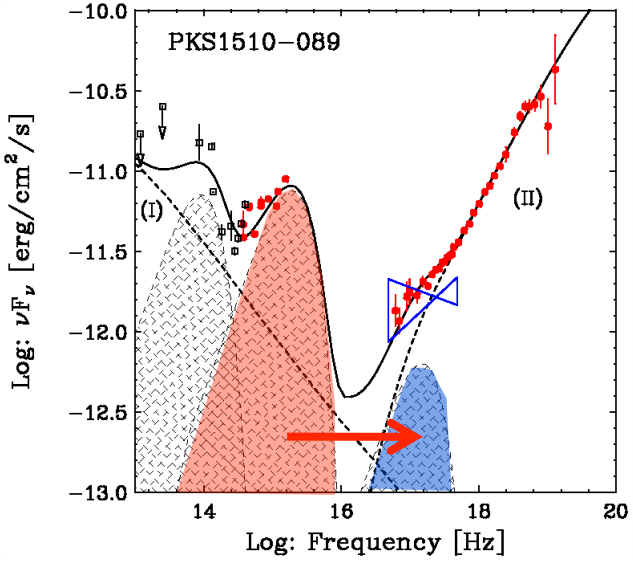

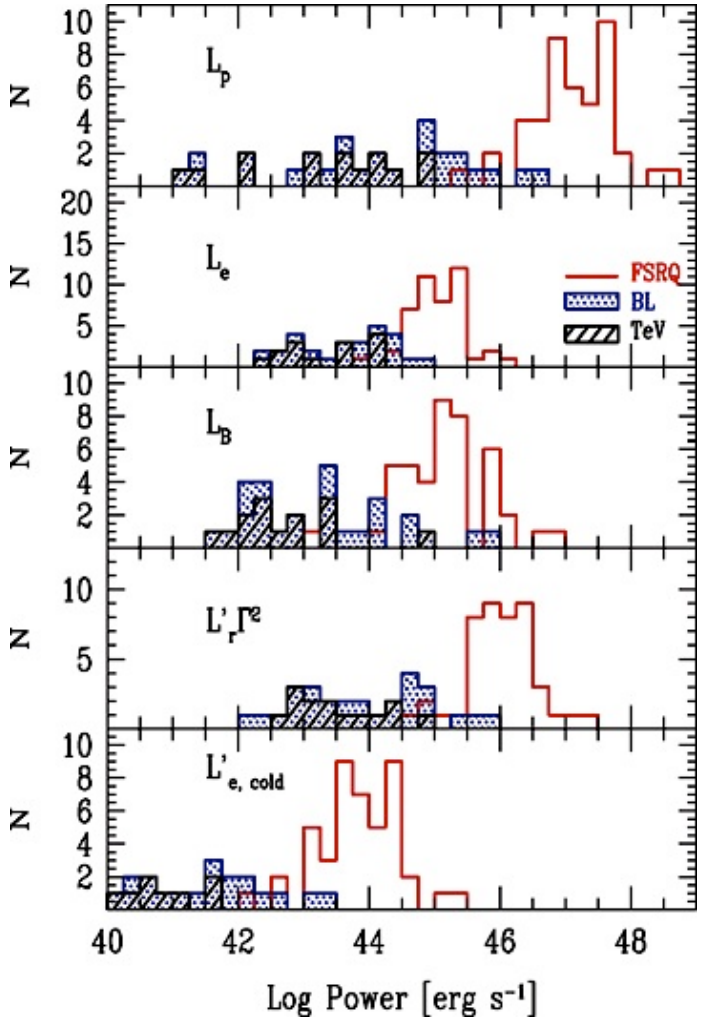

Low-Energy Electron Spectra

Table 1
Luminous Blazar Sources with the Hardest Recorded X-ray Spectra

Name (1)	z (2)	α_x (3)	α_γ^E (4)	α_γ^F (5)	Reference (6)
S5 0212+73	2.367	0.32 ± 0.19	...	...	Sambruna et al. (2007)
PKS 0229+13	2.059	0.39 ± 0.09	...	...	Marshall et al. (2005)
PKS 0413-21	0.808	0.39 ± 0.12	...	...	Marshall et al. (2005)
PKS 0528+134	2.060	0.12 ± 0.26	1.46 ± 0.04	1.54 ± 0.09	Donato et al. (2005)
PKS 0537-286	3.104	0.27 ± 0.02	1.47 ± 0.60	...	Reeves et al. (2001)
PKS 0745+241	0.409	0.35 ± 0.12	...	...	Marshall et al. (2005)
SWIFT J0746.3+2548	2.979	0.17 ± 0.01	...	...	Watanabe et al. (2009)
PKS 0805-07	1.837	0.20 ± 0.20	1.34 ± 0.29(?)	...	Giommi et al. (2007)
S5 0836+710	2.172	0.34 ± 0.04	1.62 ± 0.16	...	Donato et al. (2005)
RGB J0909+039	3.200	0.26 ± 0.12	...	...	Giommi et al. (2002)
PKS 1127-145	1.184	0.20 ± 0.03	1.70 ± 0.31	1.69 ± 0.18	Siemiginowska et al. (2008)
PKS 1424-41	1.522	0.20 ± 0.30	1.13 ± 0.21	...	Giommi et al. (2007)
GB 1428+4217	4.715	0.29 ± 0.05	...	...	Fabian et al. (1998)
PKS 1510-089	0.360	0.23 ± 0.01	1.47 ± 0.21	1.48 ± 0.05	Kataoka et al. (2008)
PKS 1830-211	2.507	0.09 ± 0.05	1.59 ± 0.13	...	De Rosa et al. (2005)
PKS 2149-306	2.345	0.38 ± 0.08	...	...	Donato et al. (2005)
PKS 2223+210	1.959	0.31 ± 0.26	...	...	Donato et al. (2005)
3C 454.3	0.859	0.34 ± 0.06	1.21 ± 0.06	1.41 ± 0.02	Donato et al. (2005)

Notes. (1) Name of a source; (2) redshift of a source, z; (3) X-ray spectral index, α_x; (4) EGRET γ-ray spectral index, α_γ^E (Hartman et al. 1999); (5) *FERMI* γ-ray spectral index, α_γ^F (Abdo et al. 2009b); and (6) references.

X-ray continua of luminous blazars of the FSRQ type, constituting low-energy segments of the inverse-Compton continua, are very flat, implying flat low-energy electron spectra with energy indices $1 < p < 2$ (Sikora et al. 09, also Tavecchio & Ghisellini 09).

Note that p=2 is often regarded as the canonical and also the "flattest" particle spectrum...

Relativistic $p^+e^\pm$ Shocks

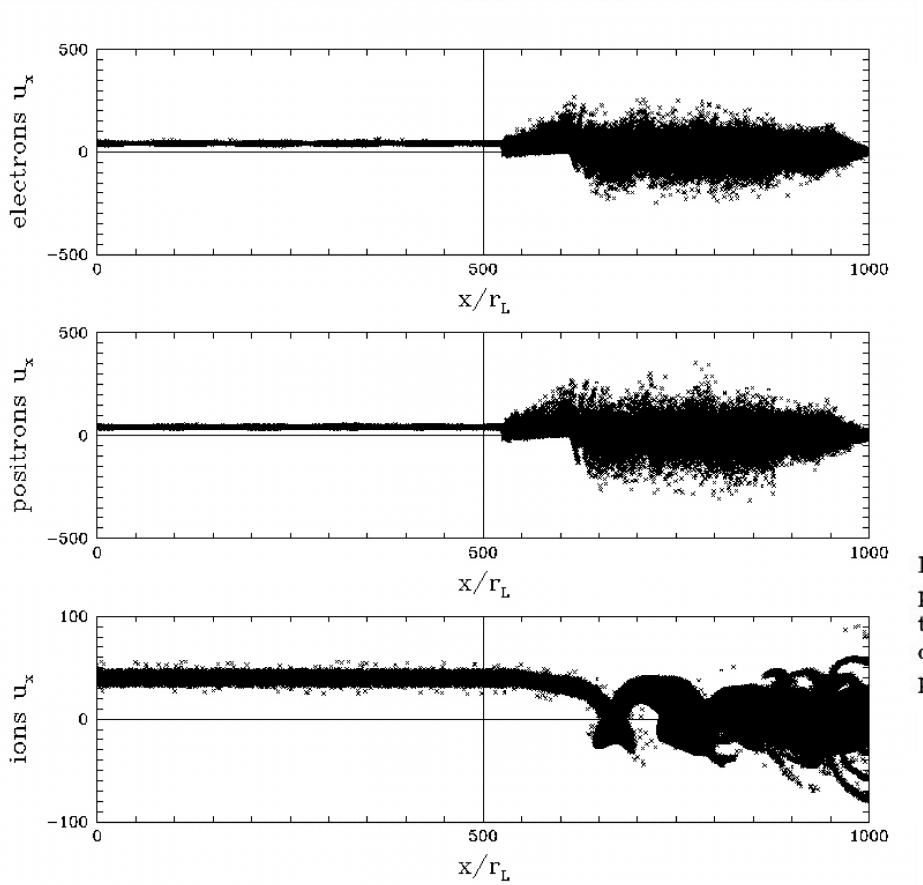

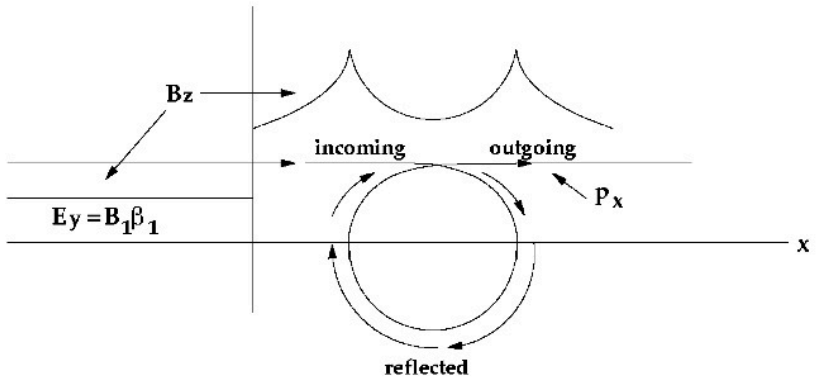

Fig. 2 Schematic representation of the leading edge of a transverse relativistic shock. The plasma drifts towards the shock front from the left. The enhancement of the magnetic field at the shock causes the particles to stop drifting and start gyrating. If the ions are energetically dominant, a further enhancement of the magnetic field intensity is produced at the reflection points of their orbits.

energy indices $p < 2$ for $E_e < E_p$

PIC simulations show that within the velocity transition region of (mildly)-relativistic, proton-mediated transverse shocks, e± with gyroradii smaller than the shock thickness (~ few times the gyroradius of background protons) can absorb electromagnetic cyclotron waves emitted at high harmonics by the protons reflected from the shock front. The resulting e± spectra are consistent with a flat ($1<p<2$) power-law between electron energies $\gamma \sim \Gamma_{sh}$ and $\gamma \sim \Gamma_{sh}\,(m_p/m_e)$ (Hoshino+ 92; Amato & Arons 06).

High-Energy Spectra

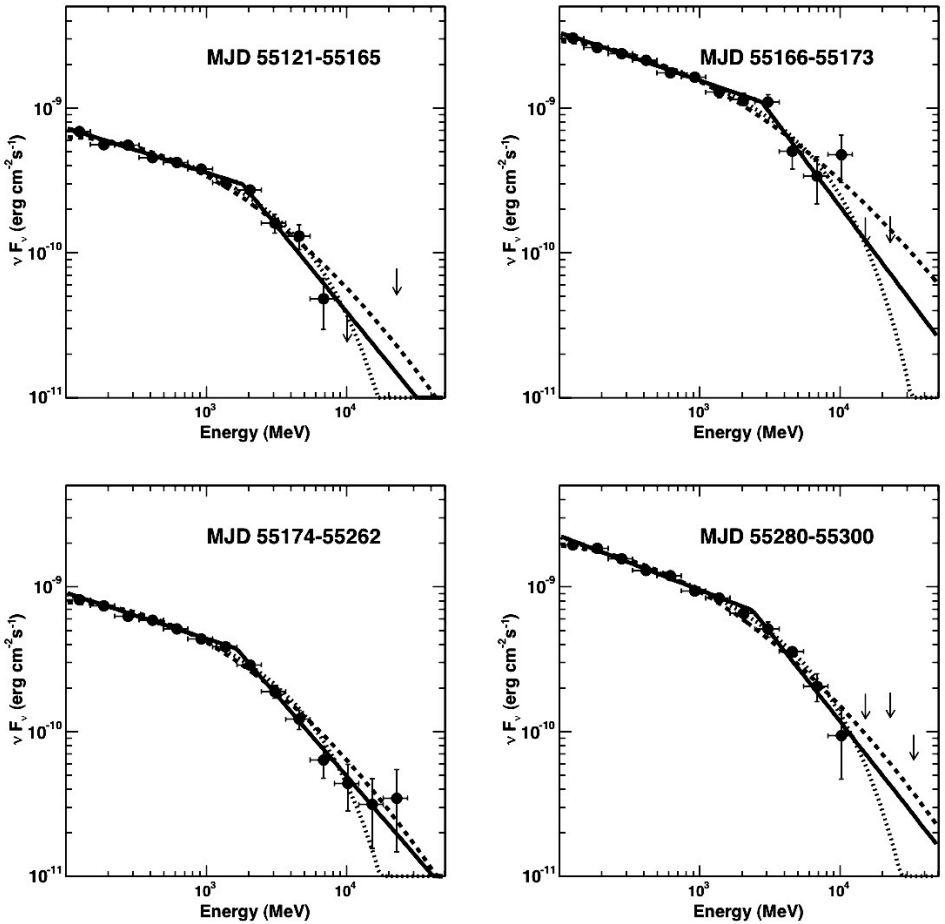

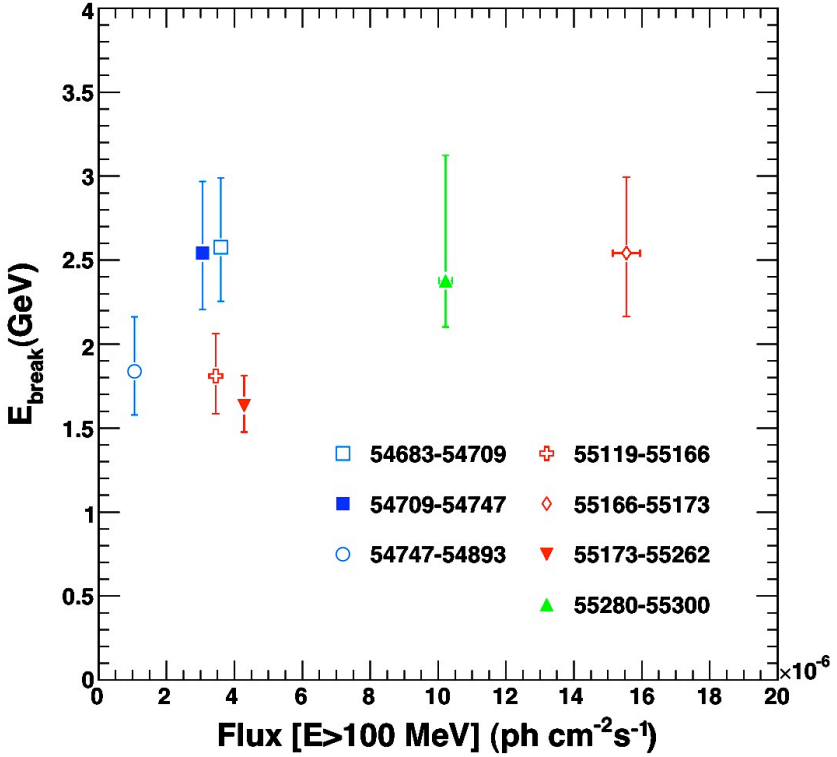

Fermi/LAT discovered that gamma-ray spectra of luminous FSRQs are typically of a broken power-law form, with spectral breaks located around the observed photon energies of a few GeV. For example, a fit between 200 MeV and 300 GeV for 3C 454.3 returns $\Gamma_1 = 2.27\pm0.03$, $\Gamma_2 = 3.5\pm0.3$, and $E_{br} = 2.4\pm0.3$ GeV (Abdo et al. 2009). Despite dramatic (hour-timescale) variability with flares up to L(>0.1GeV) ≈ 3×10^{49} erg/s, the gamma-ray spectrum seems stable (Ackermann et al. 2010).

Diffusive Shock Acceleration

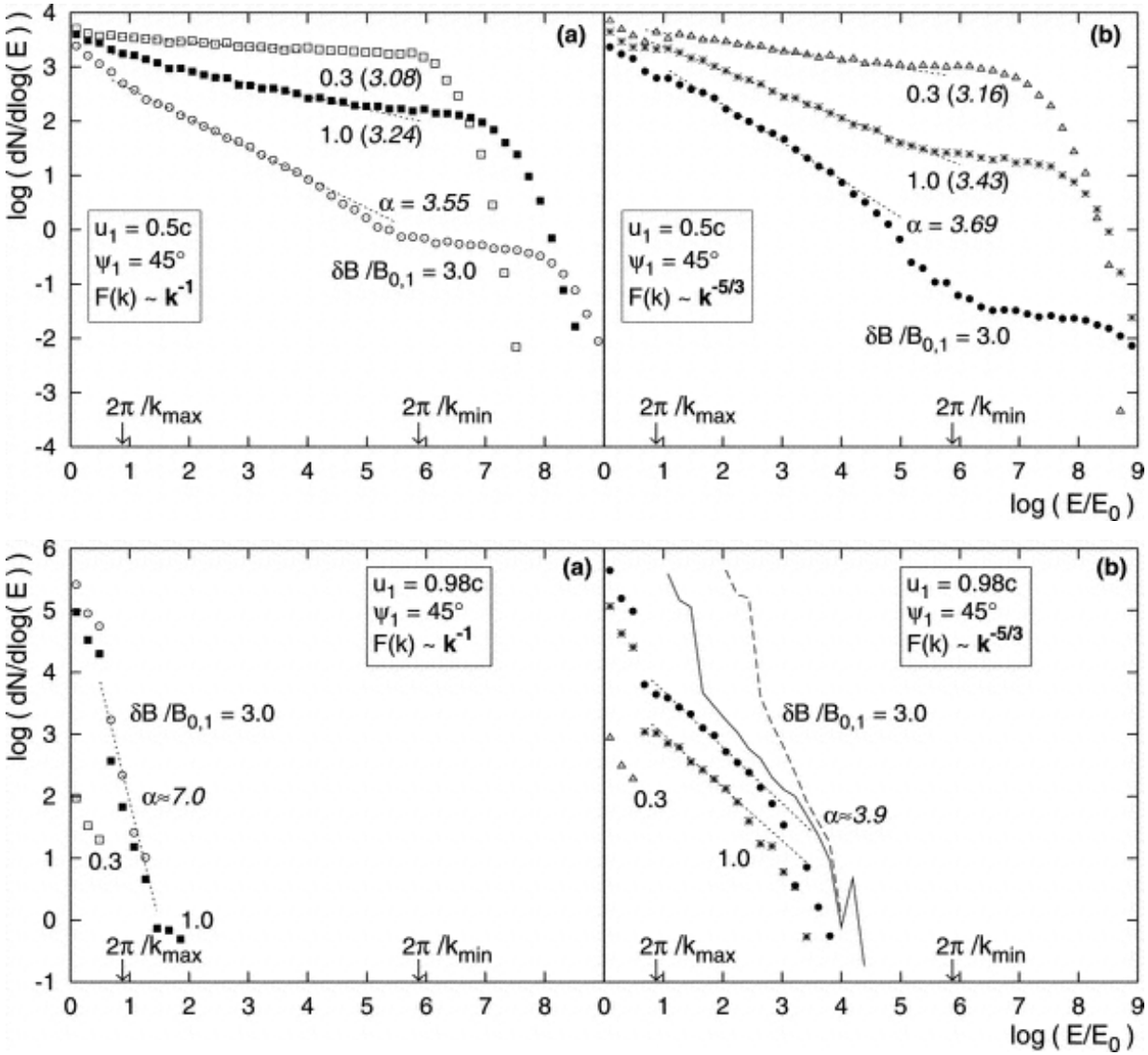

energy indices q > 2 for $E_e > E_p$

MonteCarlo simulations reveal variety of particle spectra resulting from 1st-order Fermi acceleration at relativistic shocks, depending on the magnetic field configuration (subluminal or superluminal shocks; upper and lower panels, respectively), as well as on the turbulence spectrum. Previous claims of the "universal" shock spectrum (energy index 2.2, first found by Bednarz & Ostrowski 98) were based on simulations or calculations involving very particular, possibly even unrealistic conditions (see, e.g., Ostrowski 02, Niemiec & Ostrowski 04, 06, Lemoine et al. 06).

Spectral Breaks

Tanaka et al. 11: The model involving annihilation of the GeV photons on the HeII Lyman recombination continuum and line emission of BLR clouds (Poutanen & Stern 10) may account for a break observed by Fermi/LAT in the gamma-ray spectrum of 4C+21.35. Interestingly, during its high-activity state 4C+21.35 has been also detected at 0.1-1 TeV energies by the MAGIC telescope (day-long flares; Aleksic et al. 11).

The TeV emission of 4C+21.35 is however not likely to be produced inside the zone of the highest ionization of broad line region (~10^{17} cm) due to the opacity involving IR emission of the torus. Hence the TeV photons (as well as the GeV photons, if co-spatial) have to be produced further away from the center (~10^{19} cm) in small sub-volumes of the outflow (see also Tavecchio et al. 11).

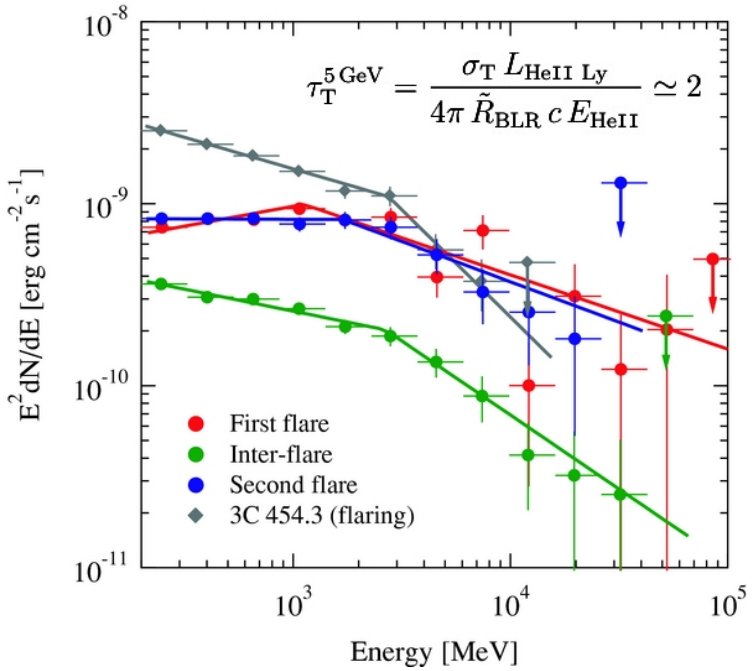

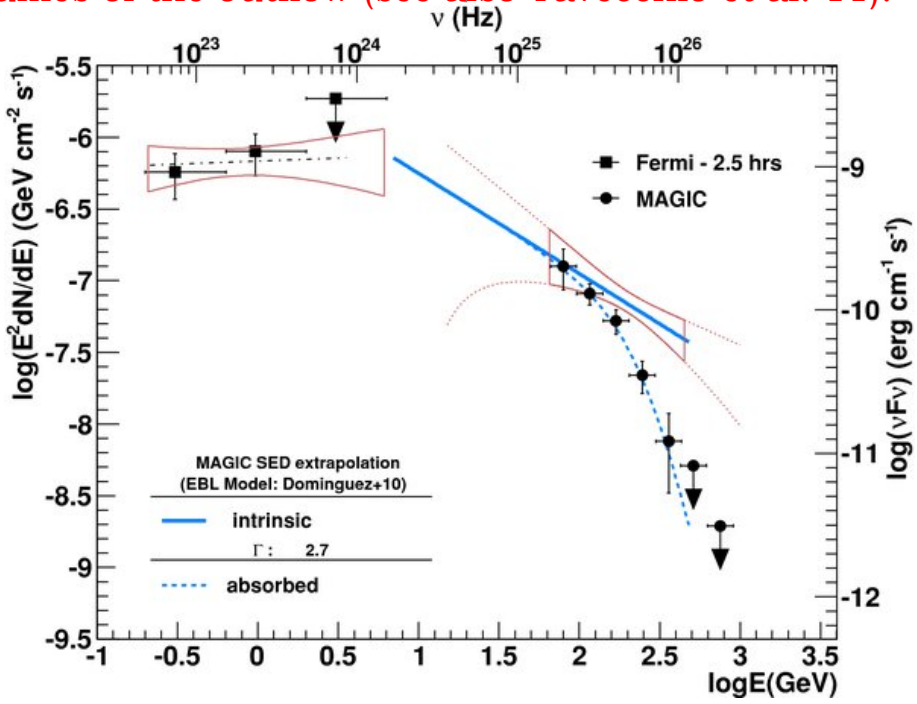

$$\frac{L_{\mathrm{jet}}}{L_{\mathrm{acc}}} \sim \left(\frac{\Gamma_{\mathrm{jet}}}{10}\right)^{-2} \left(\frac{\xi_{\mathrm{BLR}}}{0.1}\right) \left(\frac{\eta_{\mathrm{disk}}}{0.1}\right) \left(\frac{\eta_{\mathrm{jet}}}{0.1}\right)^{-1} \sim 1$$

$$\tau_{\gamma\gamma}(1\,\mathrm{TeV}) \simeq \frac{\sigma_T\, \xi_{\mathrm{HDR}}\, L_{\mathrm{disk}}}{12\pi\, R_{\mathrm{HDR}}\, c\, E_{\mathrm{HDR}}} \sim 100 \left(\frac{\xi_{\mathrm{HDR}}}{0.1}\right)$$

Elusive Variability Patterns

Abdo et al. 10
[Fermi/LAT; CAs: Hayashida & Madejski]

Coincidence of a gamma-ray flare with a dramatic change of optical polarization angle, occurring on the timescales of about ~10 days.

Non-axisymmetric structure of the emission zone is required, implying a curved trajectory for the emitting material within the jet, and the dissipation region located at a considerable distance from the black hole (almost pc-scales!)

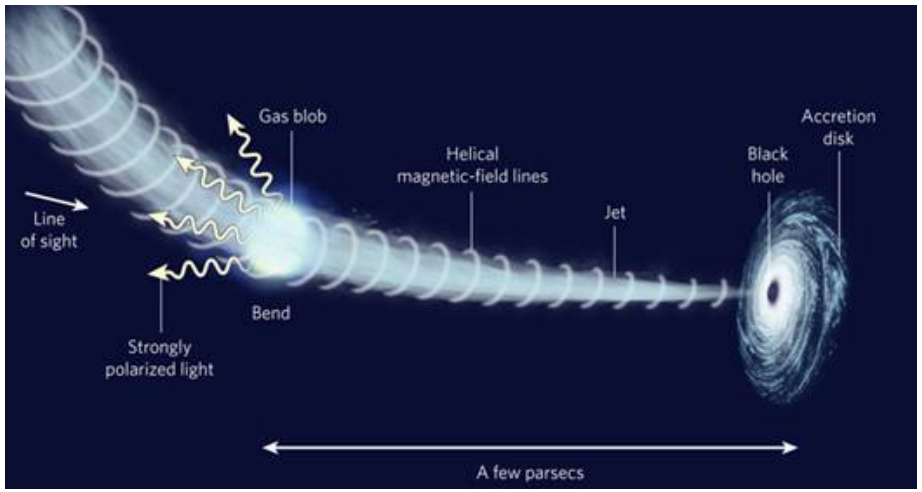

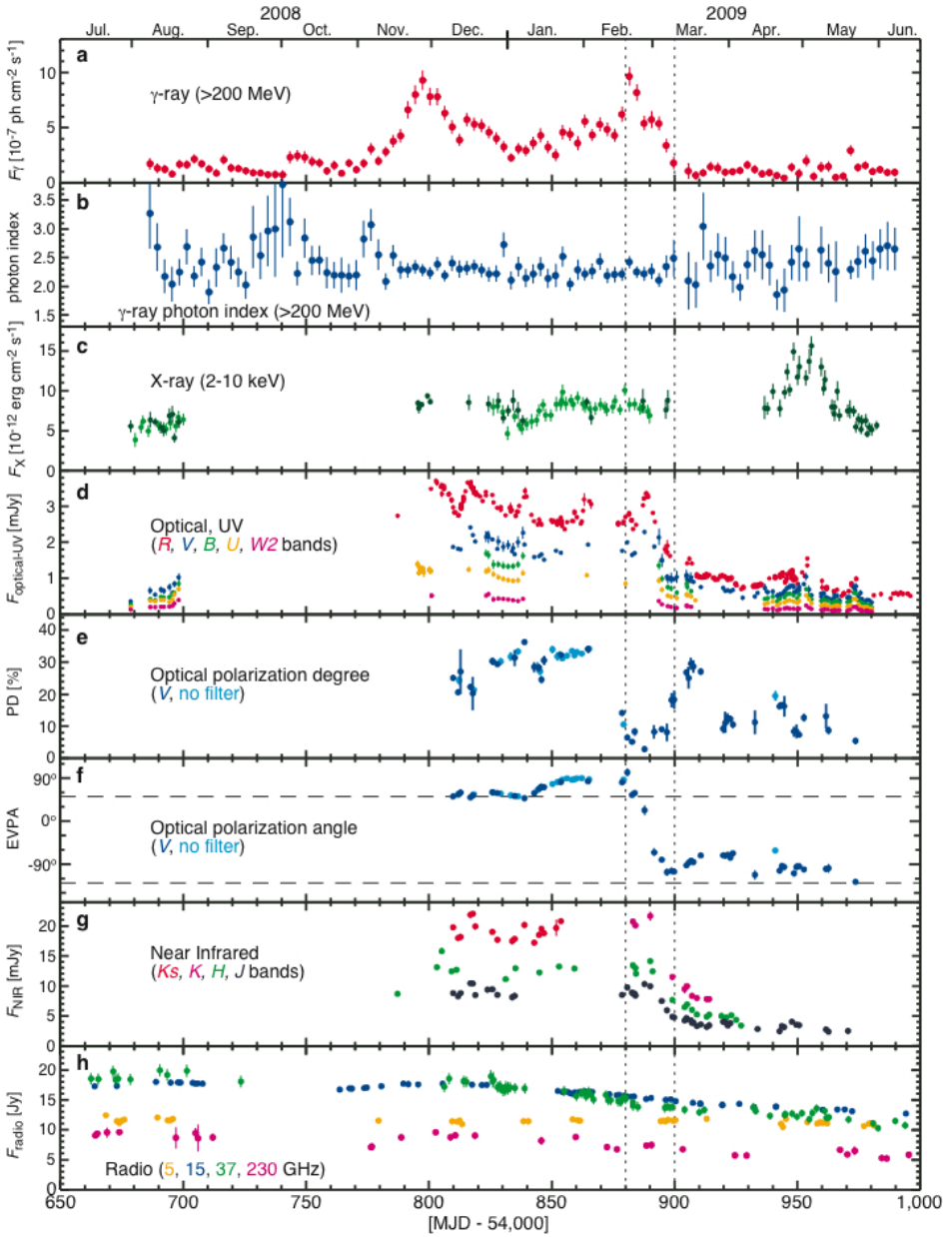

FSRQ: What We Have Learned

Jets in FSRQs are extremely powerful, carrying bulk kinetic energies comparable to the accretion (Eddington-rate) luminosities. Within the blazar emission zone about 1-10% of the total jet kinetic power in a typical FSRQ is dissipated to the internal energies of the jet particles, and radiated away predominantly in the GeV photon energy range.

- **Internal structure of relativistic jets**
  Blazar emission zone in luminous FSRQs seems to be located relatively far, around ~10^4 R_g ~ 10^{18} cm from the central engine. Yet the main emission region is not homogeneous, and consists most likely of compact sub-volumes dominating flaring activy of a source at high photon energies.

- **Jet content and energetics**
  Around the blazar emission zone, jets in FSRQs seem already matter-dominated. In addition, the total kinetic power of the outflows seems to be carried predominantly by cold, at least mildly-relativistic protons (proton-to-electron comoving number density ratio $N_{p+}/N_{e\pm}$ ~ 0.1). All the observed radiative output of FSRQs is however dominated by the synchrotron and inverse-Compton emission of ultrarelativistic electrons, and no radiative signatures of hadrons have been found.

- **Particle acceleration processes**
  Energy spectra of ultrarelativistic electrons dominating broad-band emission of FSRQs is of a multiply-broken power-law form, hardly consistent with the predictions of the 1st order Fermi acceleration at non-relativistic shocks. On the other hand, the spectra seem qualitatively consistent with the ones expected to form at relativistic, perpendicular and proton-mediated shocks.

Low-Power BL Lacs

Low-power BL Lacs are substantially different from luminous FSRQs. They accrete at low rates, and lack intense circumnuclear photon fields. BL Lacs are however extreme sources regarding maximum energies of the synchrotron and inverse-Compton photons (hard X-rays and TeV frequencies, respectively), and variability timescales.

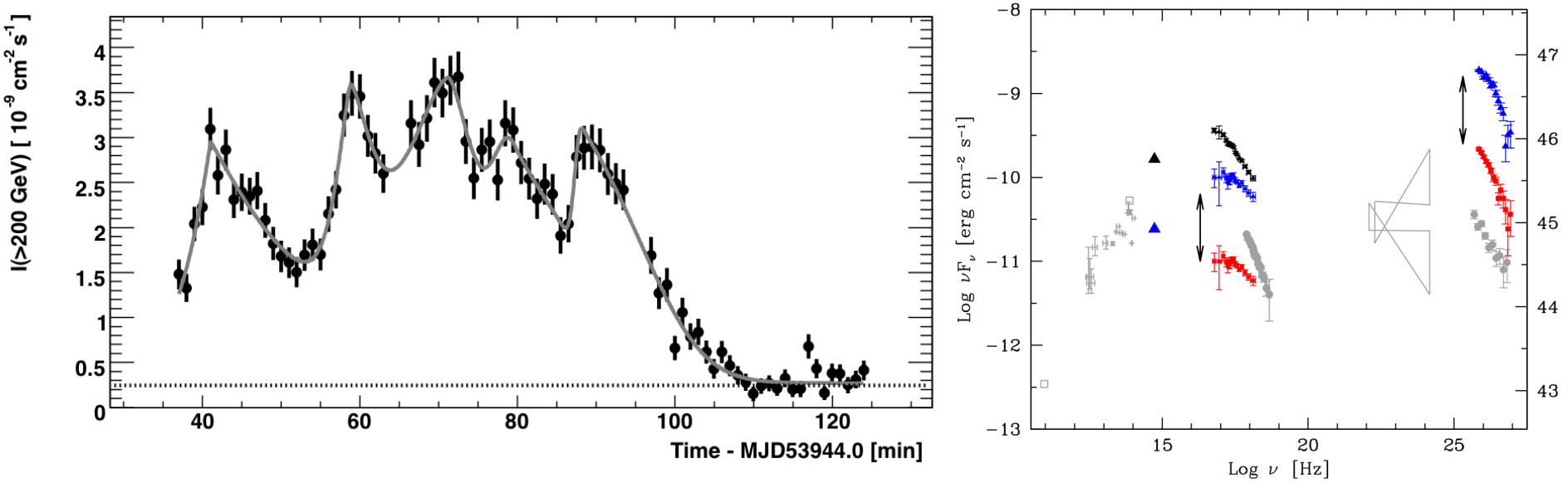

Aharonian et al. 07, 09 [HESS]: Variability in the TeV range for PKS 2155-304 is seen up to ~600 sec in the Fourier power spectrum, and well-resolved bursts varying on time scales of ~200 sec are observed. There are no strong indications for spectral variability within the data. The shortest observed flux doubling timescale, $t_{var} \sim 200$ s, implies linear size of the emitting region $R < c\, t_{var}\, \delta$. For the mass of the black hole $M_{BH} \sim 10^9\, M_{sun}$, this gives $R \sim (\delta/100) \times R_g$ suggesting that the blazar zone is located in the closest vicinity of the black hole, and that the whole outflow is already extremely relativistic thereby.

Superfast or Inhomogeneous?

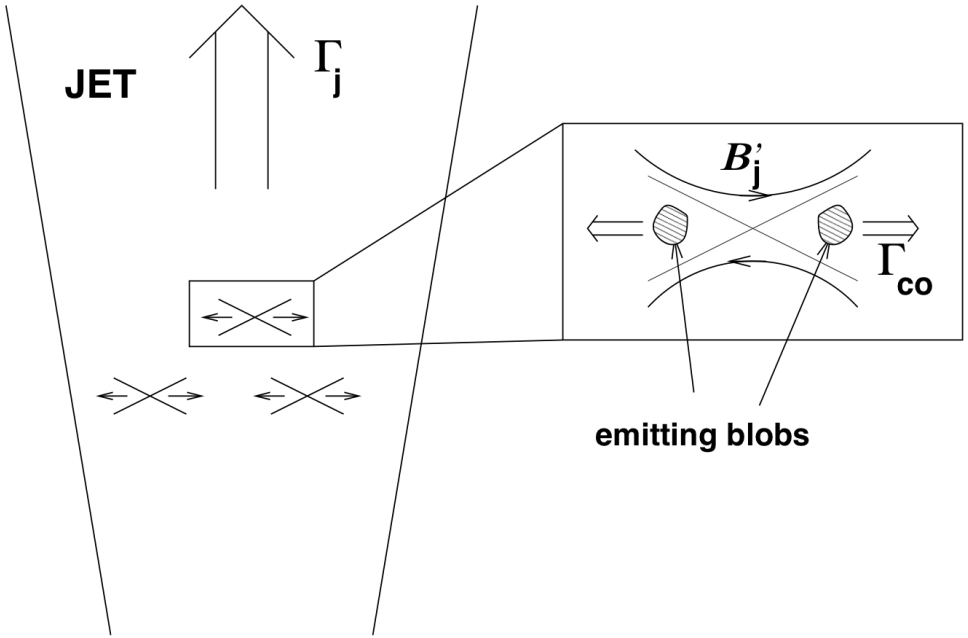

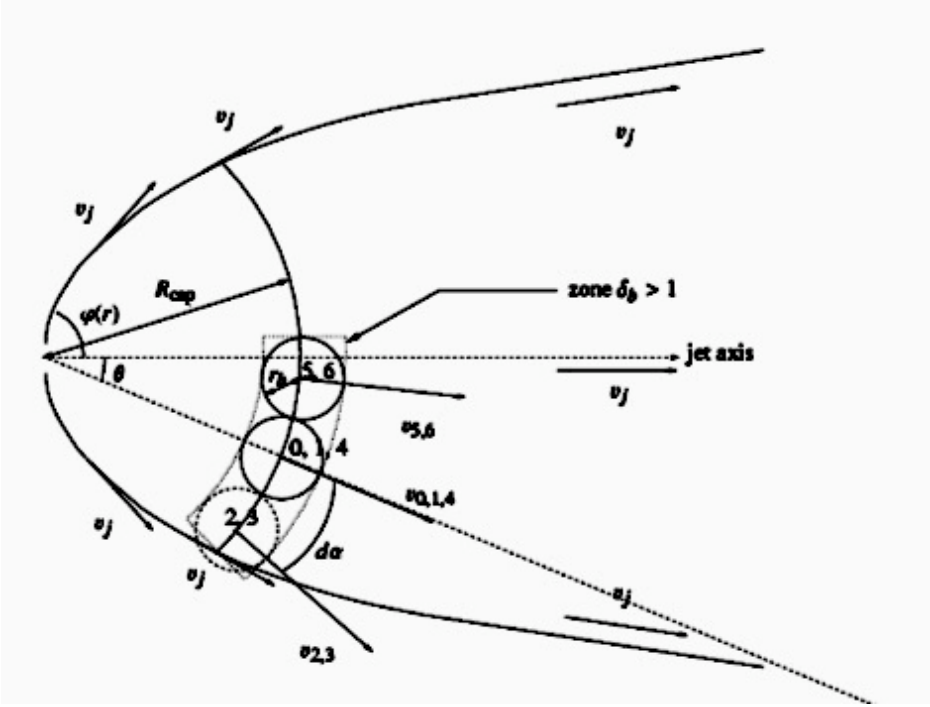

Complex pattern of broad-band flux changes observed in BL Lacs, as well as extremely short flux doubling timescales established for few of such sources (Mrk 501, PKS 2155-304), let to the emergence of inhomogeneous jet models. In the framework of these models, uncomfortably large bulk velocities of the outflows may be avoided, and the dominant emission zone, even though extremely compact, can be located at further distances from the central engine
(e.g., "jet-in-jet model", Giannios et al. 09, or "multi-blob model", Lenain et al. 08)

Curved X-ray Spectra

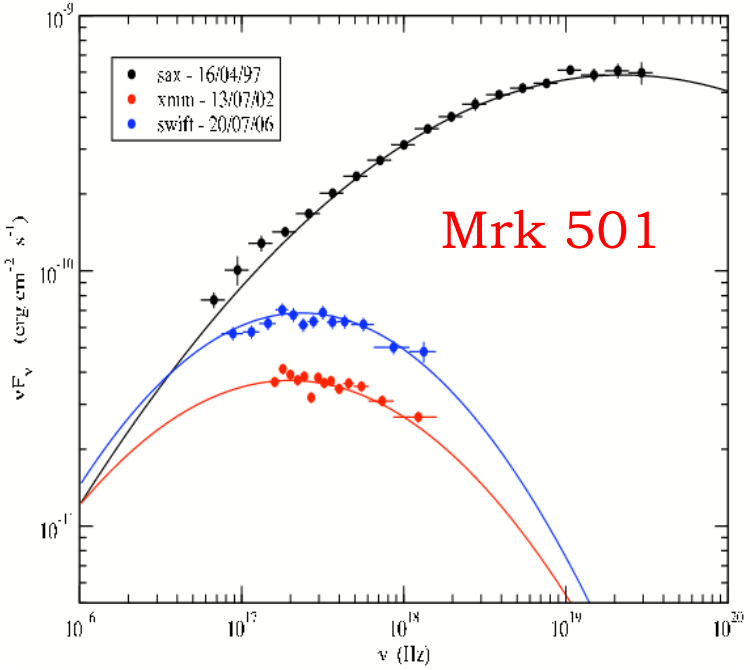

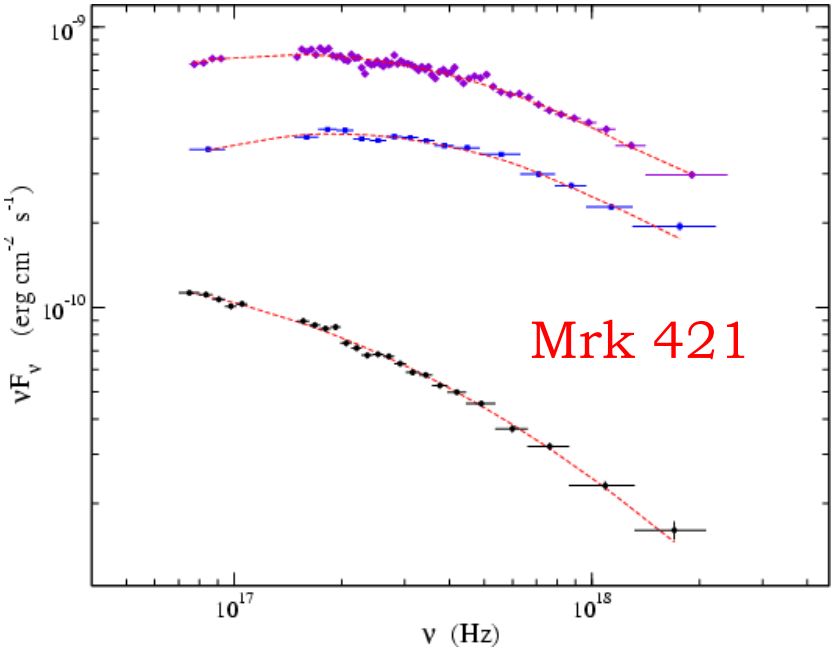

UV-to-X-ray spectra of BL Lacs are smoothly curved. They cannot be really fitted by "a power-law with an exponential cut-off" function, $F(E) \propto E^{-\Gamma} \exp(-E/E_{cr})$. Instead, "log-parabolic" shape, $F(E) \propto E^{-a + b \cdot \log(E/Ecr)}$, is claimed to represent the high-energy synchrotron continua well (Landau et al. 86, Krennrich et al. 99, Giommi et al. 02, Perri et al. 03, Massaro et al. 03, 08, Perlman et al. 05, Tramacere et al. 07).

Caution: analysis of the X-ray spectra is hampered by the hardly known intrinsic absorbing column density. In the case of BL Lacs, on the other hand, such absorption is not expected to be significant. Analysis of the optical spectra are hampered by the contribution of the elliptical host.
Caution: Synchrotron continuum due to a sharply broken power-law electron energy distribution is curved around the break frequency, and cannot be approximated very well by a broken power-law!

Ultrarelativistic Maxwellian

As long as particle escape from the acceleration region is inefficient, stochastic acceleration of ultrarelativistic particles undergoing radiative cooling $t_{rad} \propto E^x$ tends to establish modified ultrarelativistic Maxwellian spectrum

$$n_e(\gamma) = n_0 \gamma^2 \exp\left[-\frac{1}{a}\left(\frac{\gamma}{\gamma_{eq}}\right)^a\right]$$

where a = 2-q-x depending on the turbulence energy spectrum $W(k) \propto k^{-q}$, and E_{eq} is the maximum particle energy defined by the balance between the acceleration and losses timescales, $t_{acc} = t_{rad}$ (Schlickeiser 84, Henri & Pelletier 91, Park & Petrosian 95, Sauge & Henri 04, Katarzynski et al. 06, Boutellier et al. 08, Stawarz & Petrosian 08).

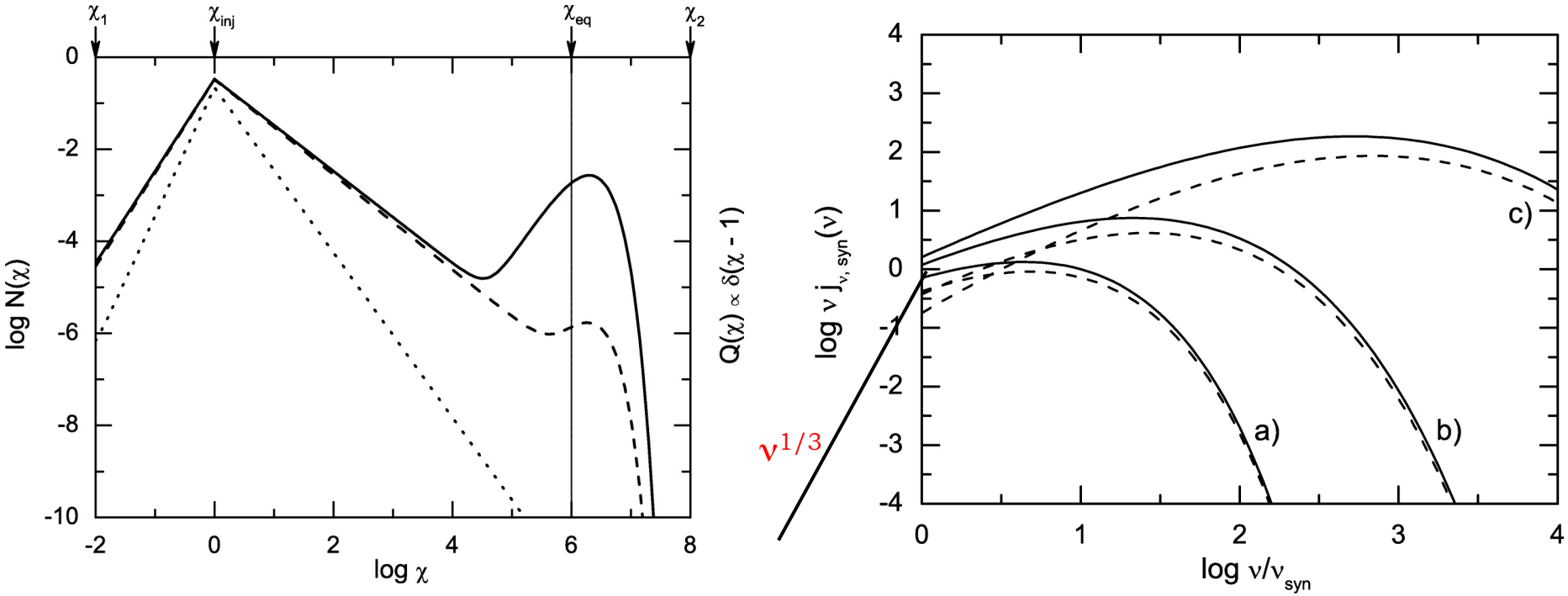

Power-Laws vs. Maxwellians

Mrk 421 during the quiescence

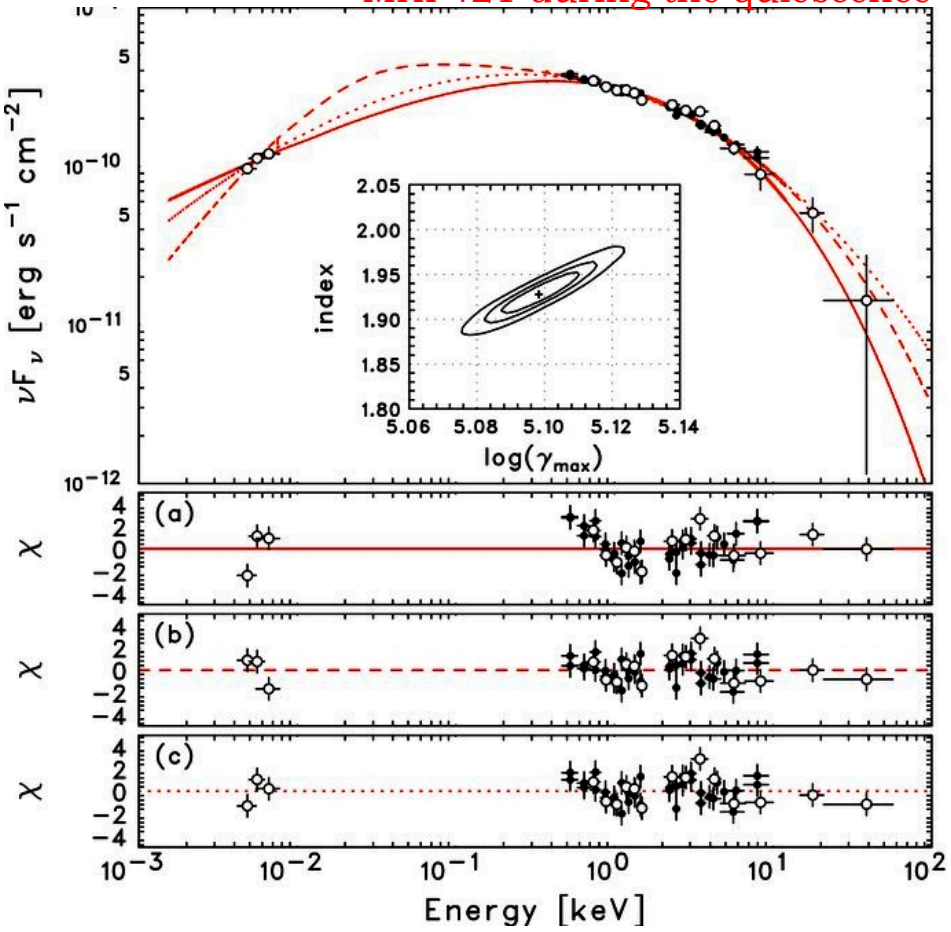

Ushio et al. 10: The broad bandpass and high-sensitivity of the Suzaku satellite enables spectral fits for the observed X-ray emission of celestial sources with synchrotron spectra originating from a given (assumed) shape of the electron energy distribution (EED), rather than by the assumed spectral form of the non-thermal emission continuum (the SYNCHROTRON model implemented to XSPEC).

In the past the analogous "parametric forward-fitting" technique has been applied in analyzing X-ray emission of solar flares (Park et al. 97, Petrosian & Chen 10).

$$\frac{dN'_e}{d\gamma} = \begin{cases} N'_0 \gamma^{-s} \exp\left[-\left(\frac{\gamma}{\gamma_{\rm max}}\right)\right] & \text{for} \quad 1 \le \gamma_{\rm min} \le \gamma \quad \text{(PL)} \\ N'_0 \gamma^{2} \exp\left[-\frac{1}{a}\left(\frac{\gamma}{\gamma_{\rm eq}}\right)^{a}\right] & \text{for} \quad 1 \le \gamma \quad \text{(UM)} \end{cases}$$

model	case	model parameters			$2-10\,$keV flux	χ^2_ν (dof)
		$\log(\gamma_{\rm min})$	$\log(\gamma_{\rm max/eq})$	s or $1/a$	$S_{2-10\,\rm keV}$ [erg cm^{-2} s^{-1}]	
PL	"a"	0.0 (fixed)	5.09 ± 0.01	$s = 1.91^{+0.01}_{-0.02}$	2.61×10^{-10}	1.86 (54)
PL	"b"	4.32 ± 0.03	$5.36^{+0.06}_{-0.05}$	$s = 2.77^{+0.13}_{-0.12}$	2.65×10^{-10}	1.12 (53)
UM	"c"	0.0 (fixed)	$1.41^{+0.06}_{-0.03}$	$1/a = 5.14^{+0.06}_{-0.09}$	2.65×10^{-10}	1.20 (54)

Massive MWL Campaigns

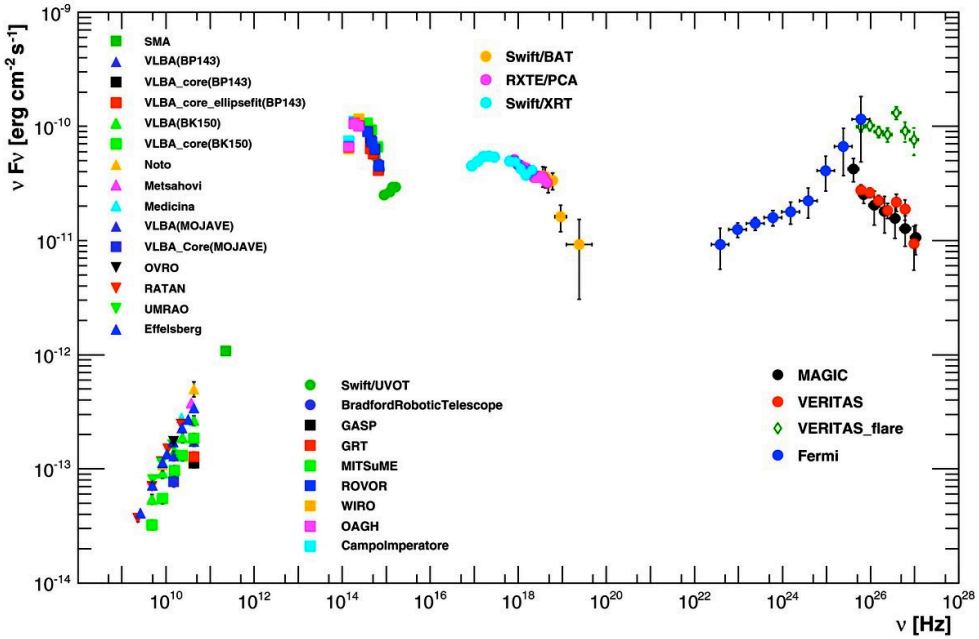

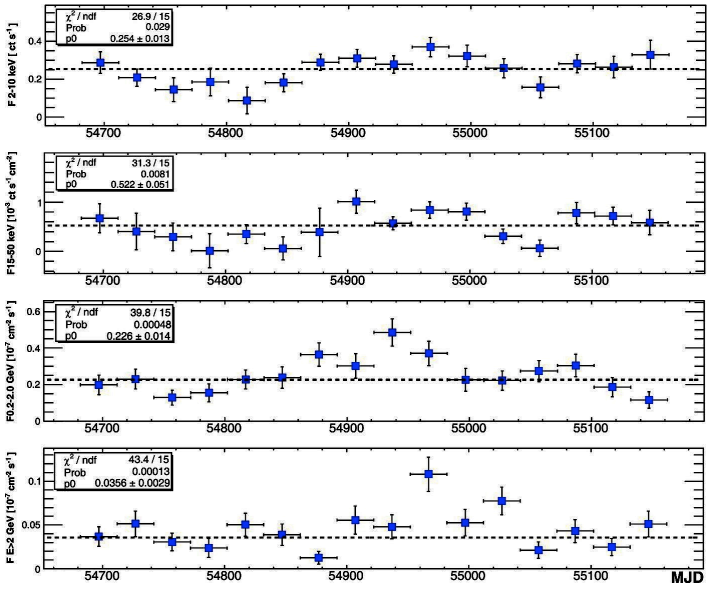

Abdo et al 10 [Fermi/LAT, VERITAS & Magic++; CAs: Paneque & Stawarz]

Truly multiwavelength and simultaneous observations of Mrk 501 with the best (up to date) spatial and temporal coverage.

The "typical" behavior of Mrk 501: only modest and rather long-timescale flux changes

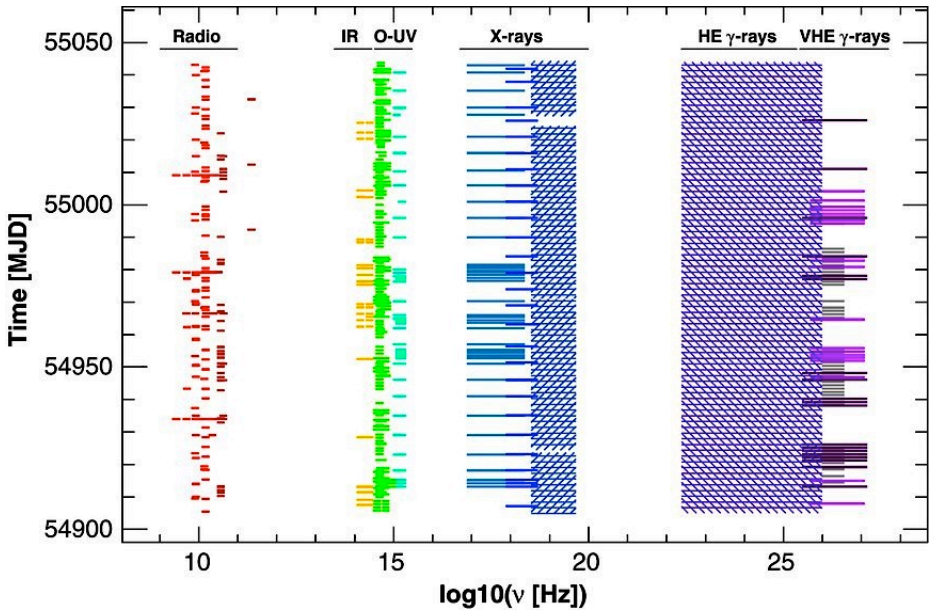

SSC Modeling

Table 2. Parameters of the blazar emission zone in Mrk 501.

Parameter	Main SSC fit considered
Magnetic field	$B = 0.015\,\mathrm{G}$
Emission region size	$R = 1.3 \times 10^{17}\,\mathrm{cm}$
Jet Doppler and bulk Lorentz factors	$\Gamma = \delta = 12$
Equipartition parameter	$\eta_e \equiv U'_e/U'_B = 56$
Minimum electron energy	$\gamma_{min} = 600$
Intrinsic electron break energy	$\gamma_{br,1} = 4 \times 10^4$
Cooling electron break energy	$\gamma_{br,2} = 9 \times 10^5$
Maximum electron energy	$\gamma_{max} = 1.5 \times 10^7$
Low-energy electron index	$s_1 = 2.2$
High-energy electron index	$s_2 = 2.7$
Electron index above the cooling break	$s_3 = 3.65$
Mean electron energy	$\langle\gamma\rangle \simeq 2400$
Main variability timescale	$t_{var} \simeq 4\,\mathrm{day}$
Comoving electron energy density	$U'_e \simeq 0.5 \times 10^{-3}\,\mathrm{erg\,cm^{-3}}$
Comoving magnetic field energy density	$U'_B \simeq 0.9 \times 10^{-5}\,\mathrm{erg\,cm^{-3}}$
Comoving energy density of synchrotron photons	$U'_{syn} \simeq 0.9 \times 10^{-5}\,\mathrm{erg\,cm^{-3}}$
Comoving electron number density	$N'_e \simeq 0.3\,\mathrm{cm^{-3}}$
Luminosity of the host galaxy	$L_{star} \simeq 3 \times 10^{44}\,\mathrm{erg\,s^{-1}}$
Jet power carried by electrons	$L_e \simeq 1.1 \times 10^{44}\,\mathrm{erg\,s^{-1}}$
Jet power carried by magnetic field	$L_B \simeq 2 \times 10^{42}\,\mathrm{erg\,s^{-1}}$
Jet power carried by protons[a]	$L_p \simeq 3 \times 10^{43}\,\mathrm{erg\,s^{-1}}$
Total jet kinetic power	$L_j \simeq 1.4 \times 10^{44}\,\mathrm{erg\,s^{-1}}$
Total emitted power	$L_{em} \simeq 9.7 \times 10^{42}\,\mathrm{erg\,s^{-1}}$
Isotropic synchrotron luminosity	$L_{syn} \simeq 10^{45}\,\mathrm{erg\,s^{-1}}$
Isotropic SSC luminosity	$L_{ssc} \simeq 2 \times 10^{44}\,\mathrm{erg\,s^{-1}}$

Abdo et al 10 [Fermi/LAT, VERITAS & Magic++; CAs: Paneque & Stawarz]

$$n'_e(\gamma) \propto \begin{cases} \gamma^{-s_1} & \text{for} \quad \gamma_{min} \le \gamma < \gamma_{br,1} \\ \gamma^{-s_2} & \text{for} \quad \gamma_{br,1} \le \gamma < \gamma_{br,2} \\ \gamma^{-s_3}\,\exp\left[-\gamma/\gamma_{max}\right] & \text{for} \quad \gamma_{br,2} \le \gamma \end{cases}$$

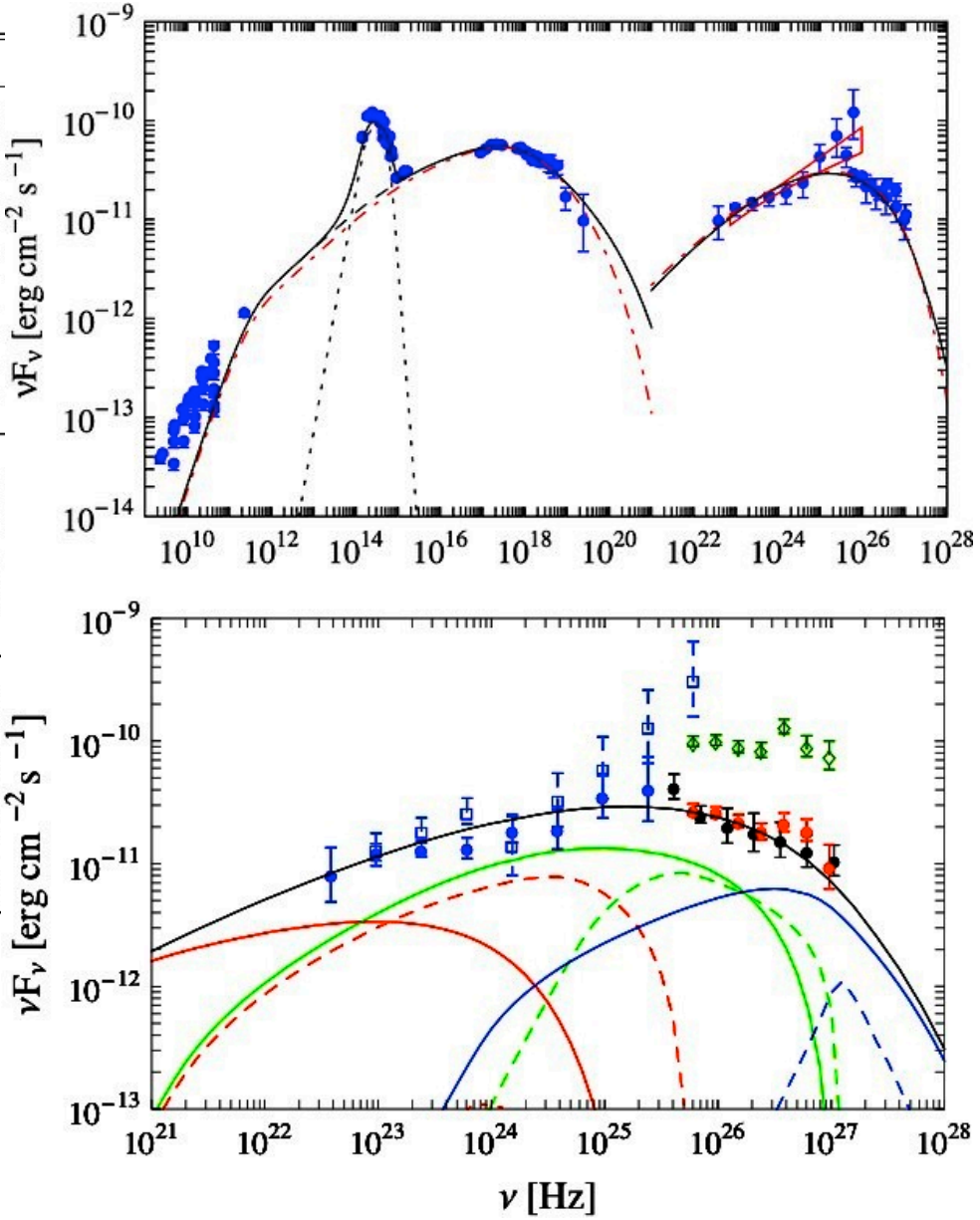

Dominant Emission Site

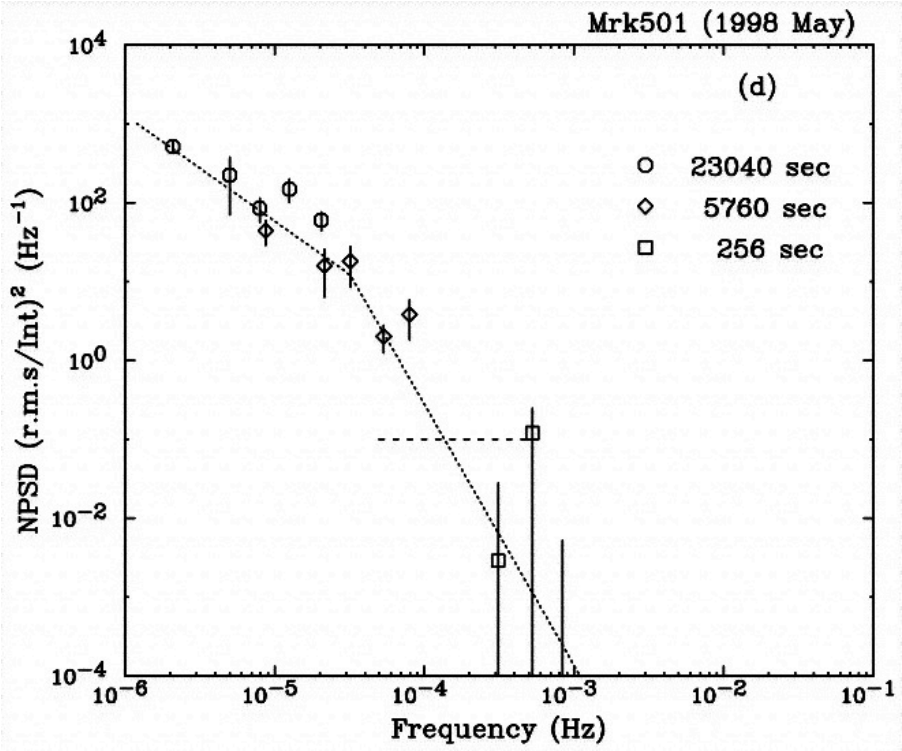

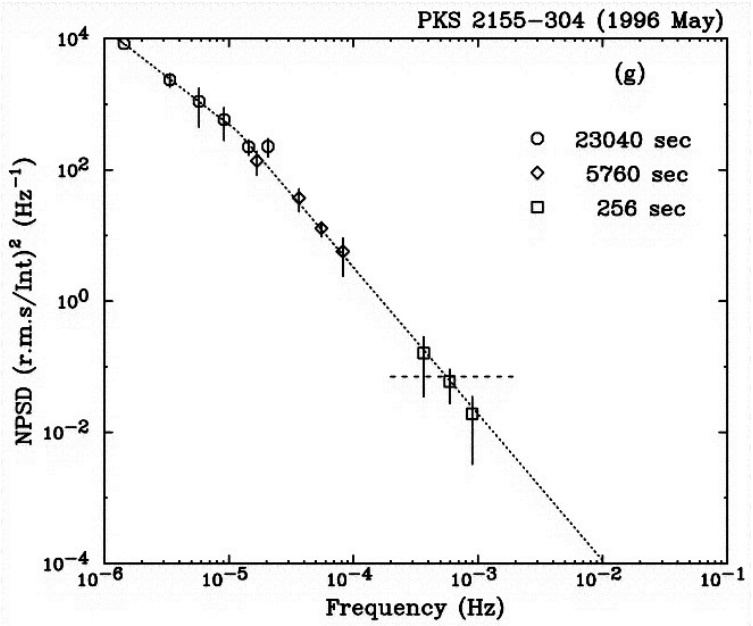

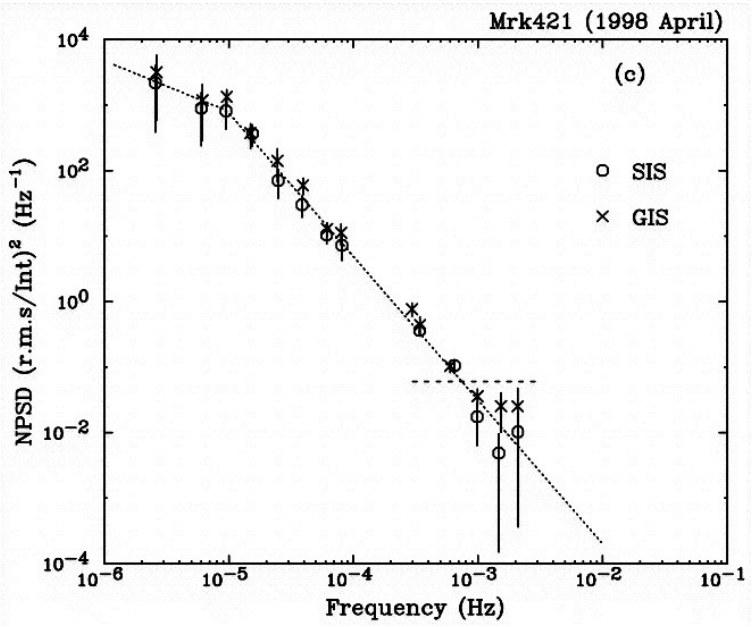

Kataoka et al. 01: Analysis of the X-ray light curves for several bright BL Lacs (variability in the time domain from 10^3 to 10^8s.

Both the power spectrum density and the structure function show a roll-over with a time-scale of the order of 1 day or longer. On time-scales shorter than 1 day, there is only small power in the variability. Thus, the dominant X-ray emitting site in the jet seems to be located at $>10^{17}$ cm distances from the base of the core.

BL Lacs: What We Have Learned

Jets in BL Lacs are extremely efficient and fast particle accelerators. Within the blazar emission zone, electrons can be accelerated on the timescales of minutes and hours to maximum energies of the order of 10-100 TeV. The flaring duty cycle of BL Lacs is on the other hand quite modest, at the level of 1% on average.

- **Internal structure of relativistic jets**
  Blazar emission zone in low-power BL Lacs remains elusive. It seems that most of the energy is dissipated relatively far from the central engine, at the scales $>10^{17}$ cm. Rapid and rare high-energy flares may originate either extremely close to supermassive black holes, or further away, within extremely compact sub-volumes of the outflows.

- **Jet content and energetics**
  Around the blazar emission zone, jets in BL Lacs seem already matter-dominated. All their observed radiative output can be well explained by the synchrotron and inverse-Compton emission of ultrarelativistic electrons, and no radiative signatures of hadrons have been found. Jet content in BL Lacs remains and open issue.

- **Particle acceleration processes**
  Energy spectra of ultrarelativistic electrons dominating broad-band emission of BL Lacs are well approximated by a multiply-broken power-law form, at least during the quiescence states. The alternative spectral shapes (ultrarelativistic Maxwellians, for example) are still allowed, though in principle not needed (with a possible exception of flaring states, which are hardly explored and covered across the electromagnetic continuum, and which may involve “non-standard” particle spectra and acceleration processes alternative to the shock acceleration).

M87: Misaligned Blazar

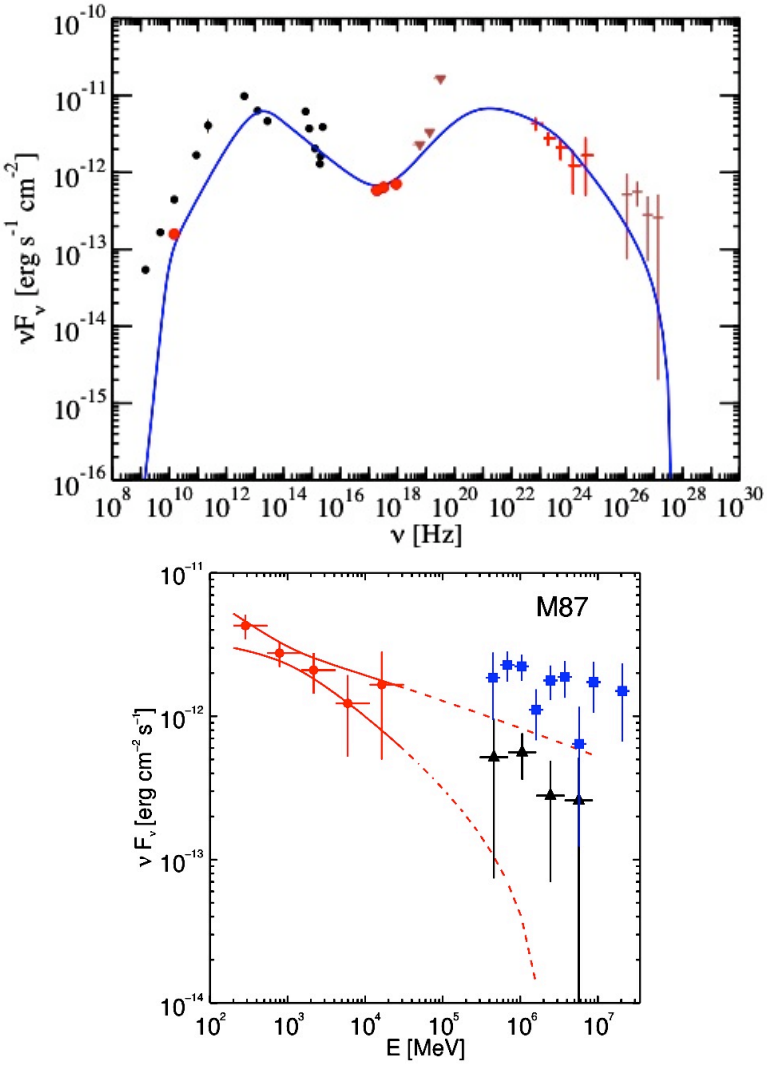

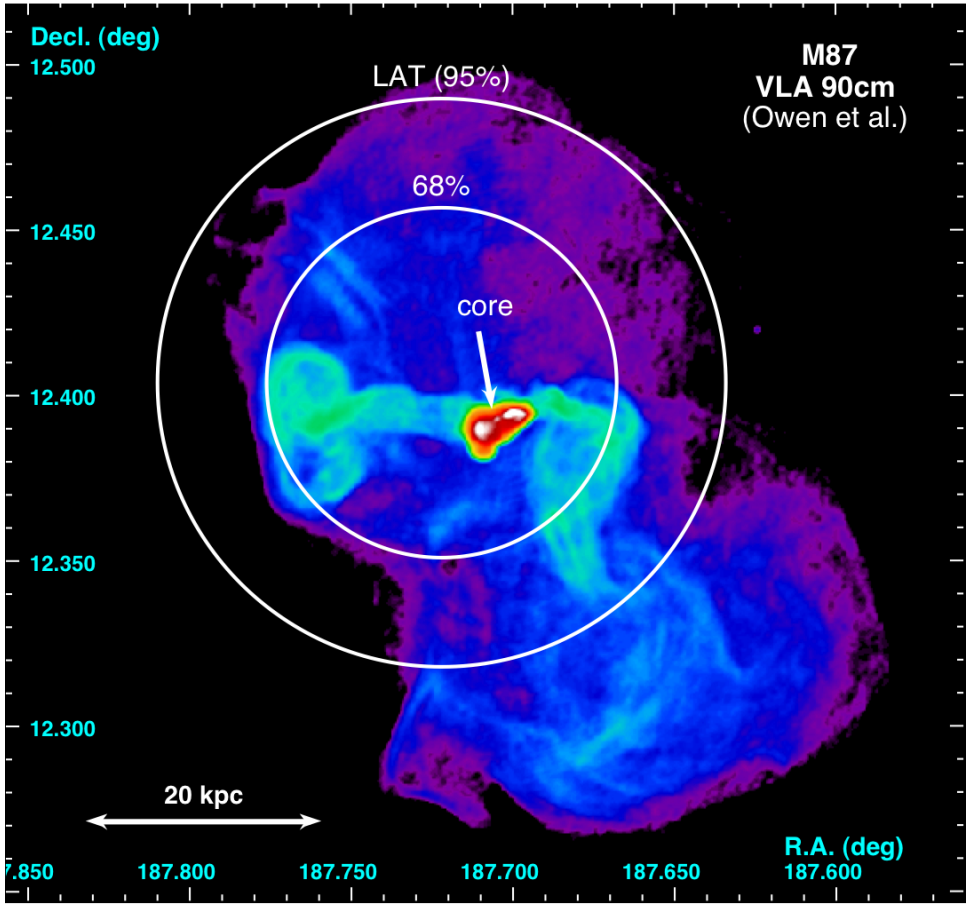

M 87 radio galaxy detected at GeV and TeV photon energies (Aharonian et al. 06, Acciari et al. 08, Albert et al. 08, Abdo et al. 2009; HESS< MAGIC, VERITAS, Fermi/LAT). Due to its proximity (about 17 Mpc), the jet in M87 can be resolved at radio frequencies down to ~100 R_g scales.

Where Is The Blazar Zone?

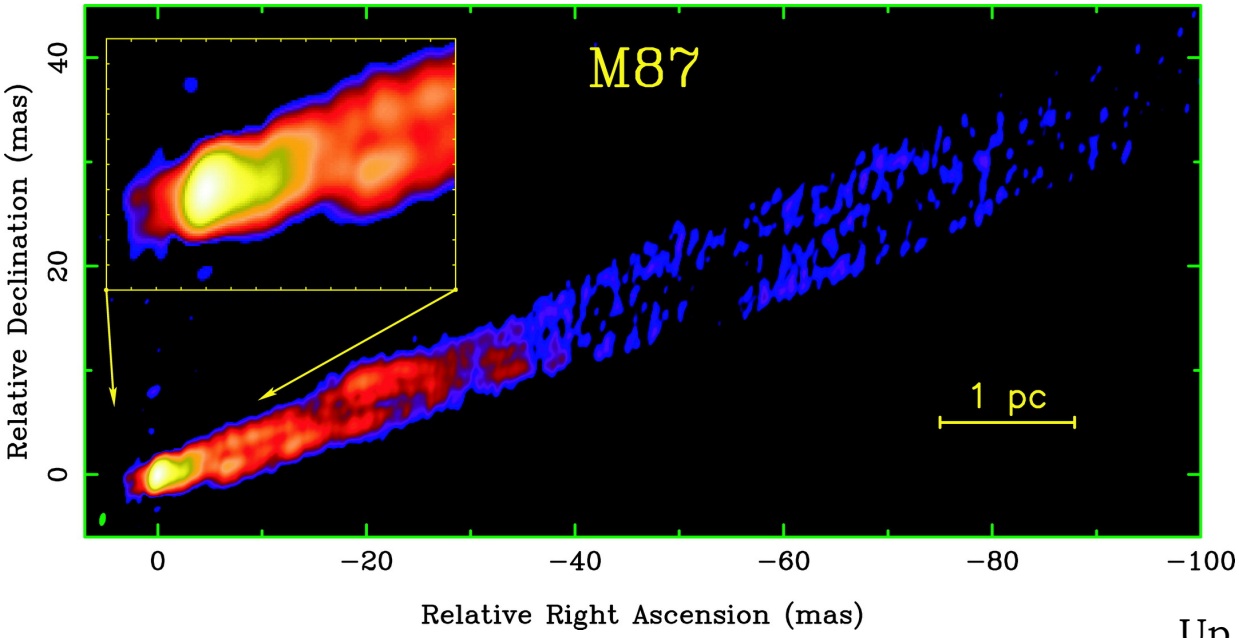

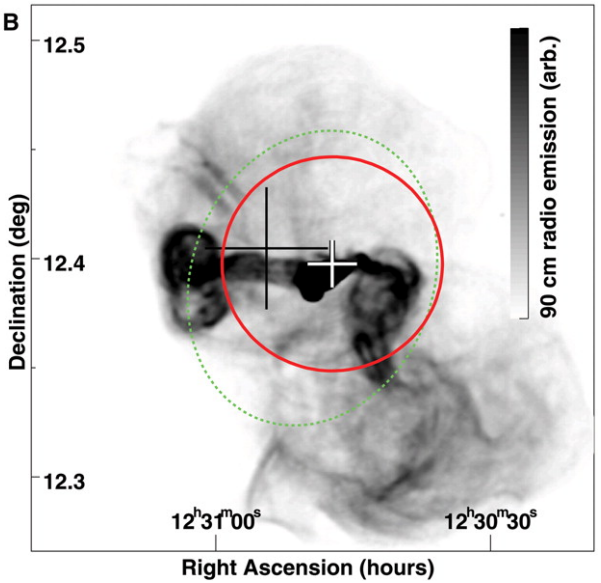

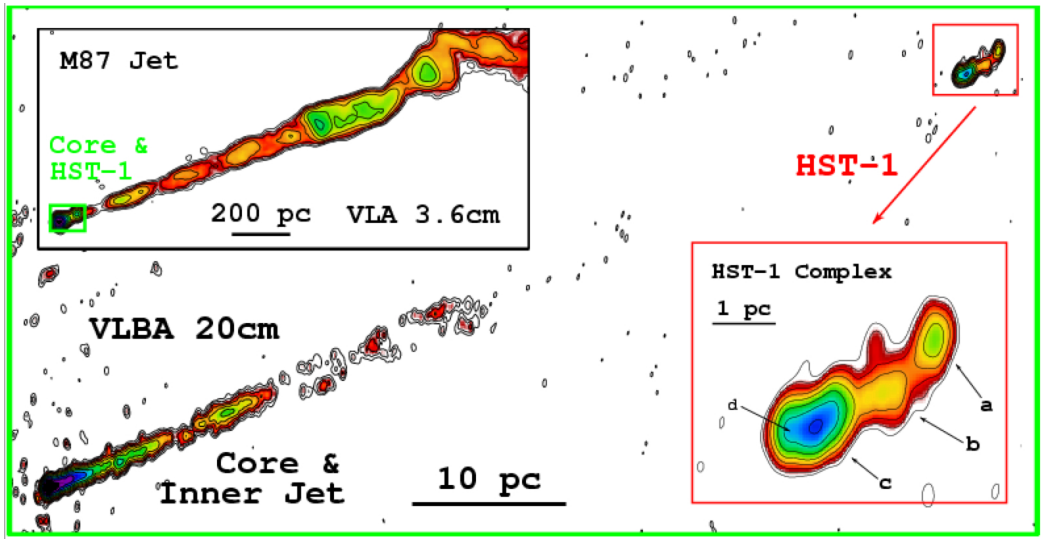

Up to ~100 pc distances from the M87 nucleus we see almost featureless, limb-brightened, slowly collimating outflow (e.g., Kovalev et al. 2007).

Around 100pc (~10^6 r_g) from the nucleus, compact (unresolved), stationary, and variable feature HST-1 is observed in radio, optical, and X-rays (Harris et al. 03/09).

Downstream of HST-1, superluminal blobs have been detected (Biretta et al. 99, Cheung et al. 07).

HST-1 Knot

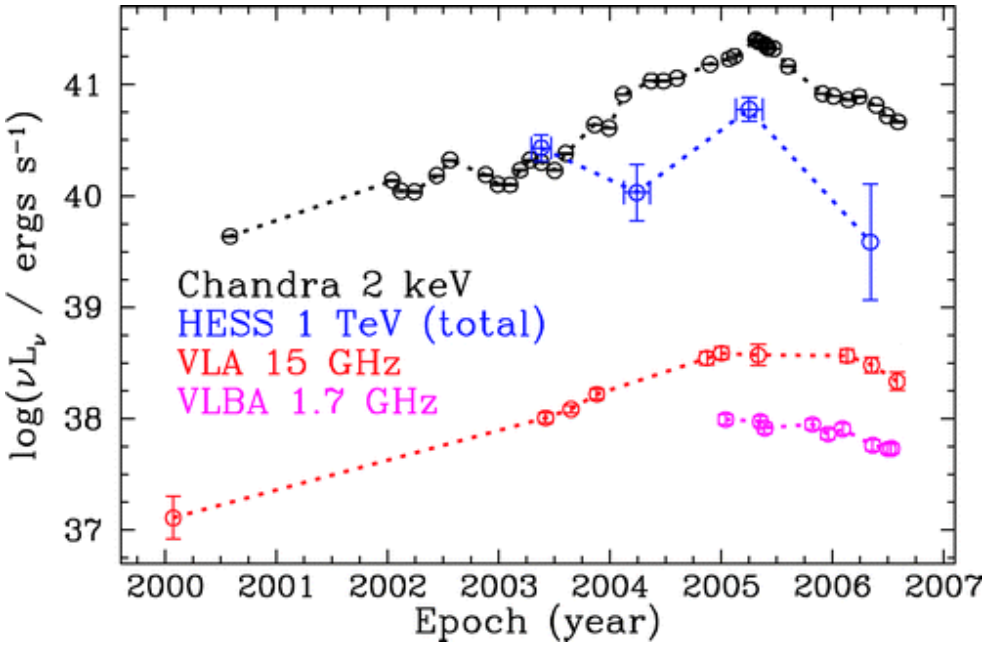

Cheung et al. 07: In 2003-07, the TeV outburst of M87 coincided with the radio-to-X-ray flare of HST-1 knot. Around the maximum of the flare, stationary HST-1 knot ejected superluminal radio blobs ($v_{app} \leq 4$ c).

TeV emission: day variability. Radio, optical, X-ray emission of HST-1 knot: weeks/month variability.

HST-1 knot may be understood as a nozzle formed by a converging reconfinement shock (Stawarz et al. 06, Gracia et al. 09, Bromberg & Levinson 09, Nakamura et al. 10)

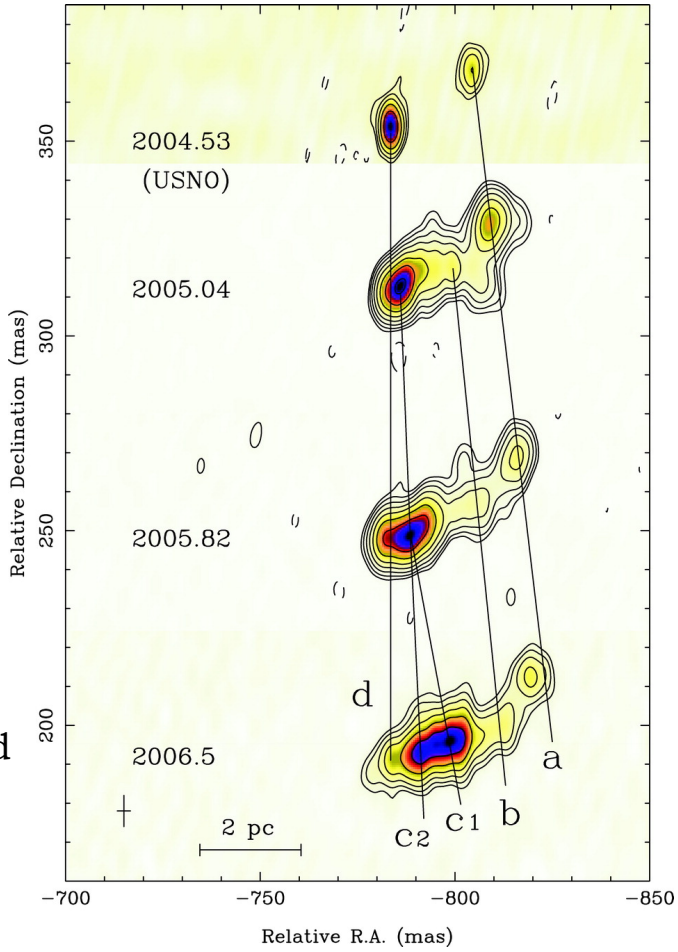

r ~ 100 pc

$R_{HST} < 0.2$ pc

$R_X < 0.02\ \delta$ pc

$R_{TeV} < 0.002\ \delta$ pc

Unresolved Nucleus

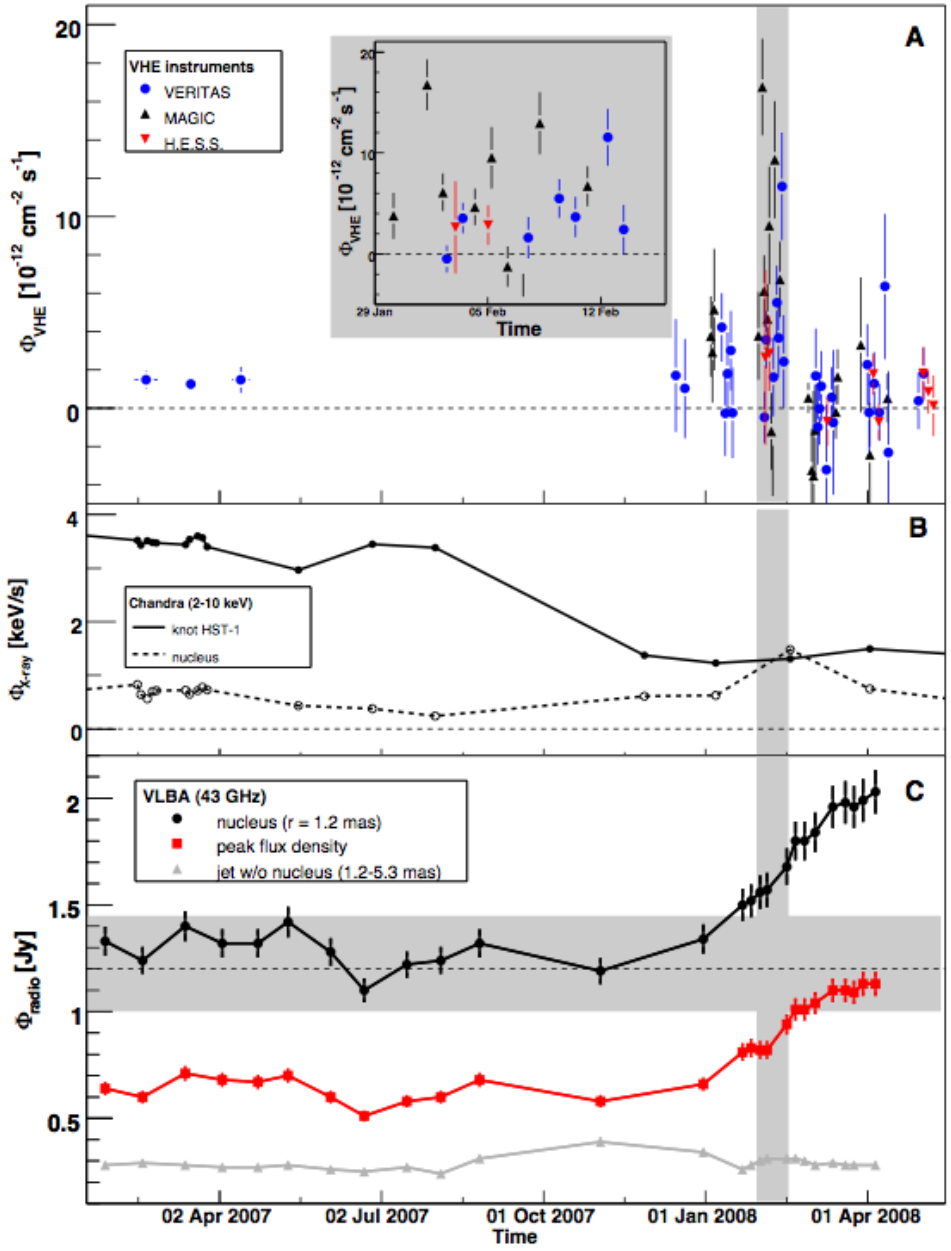

Acciari et al. 09: the 2008 TeV flare did not coincide with any enhanced activity of the HST-1 knot , but instead of the nucleus (radio and X-ray frequencies)

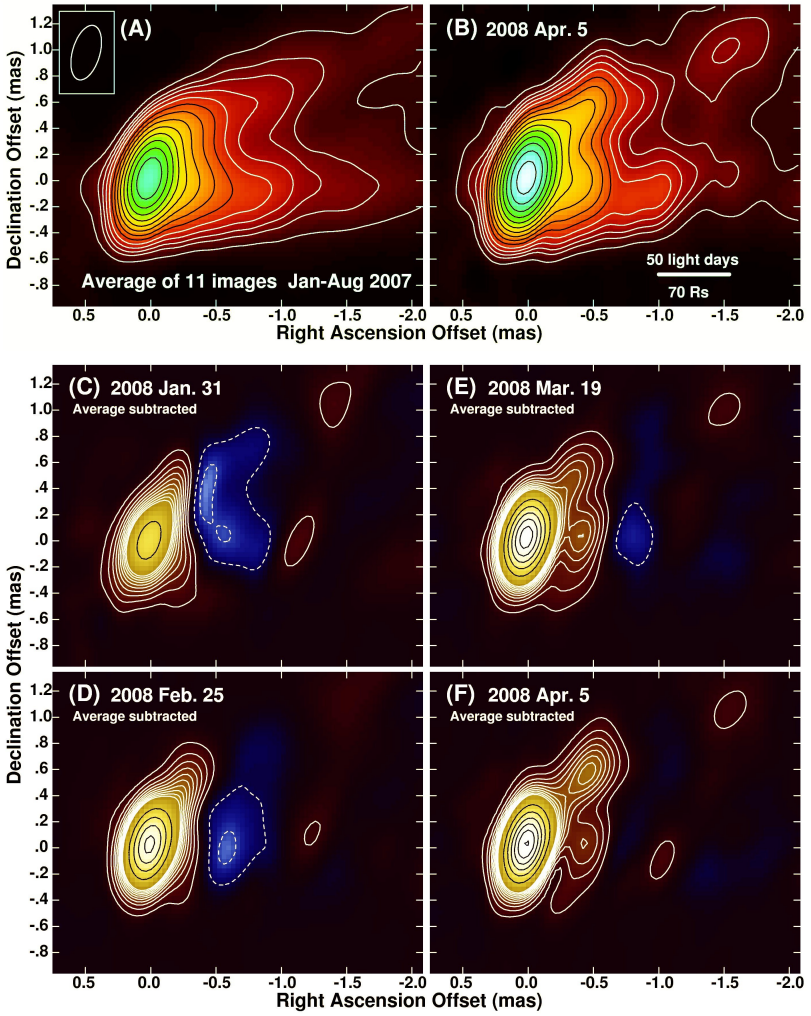

MWL M87

2010 M87 Campaign

[Preliminary results presented by M. Raue et al. on behalf of the HESS, VERITAS, Magic, Fermi/LAT++ joint collaboration during the HEPRO III meeting in Barcelona, Spain (27-30.06. 2011), and in Muonio, Finland (11-15.04.2011). Joint paper to be submitted soon.]

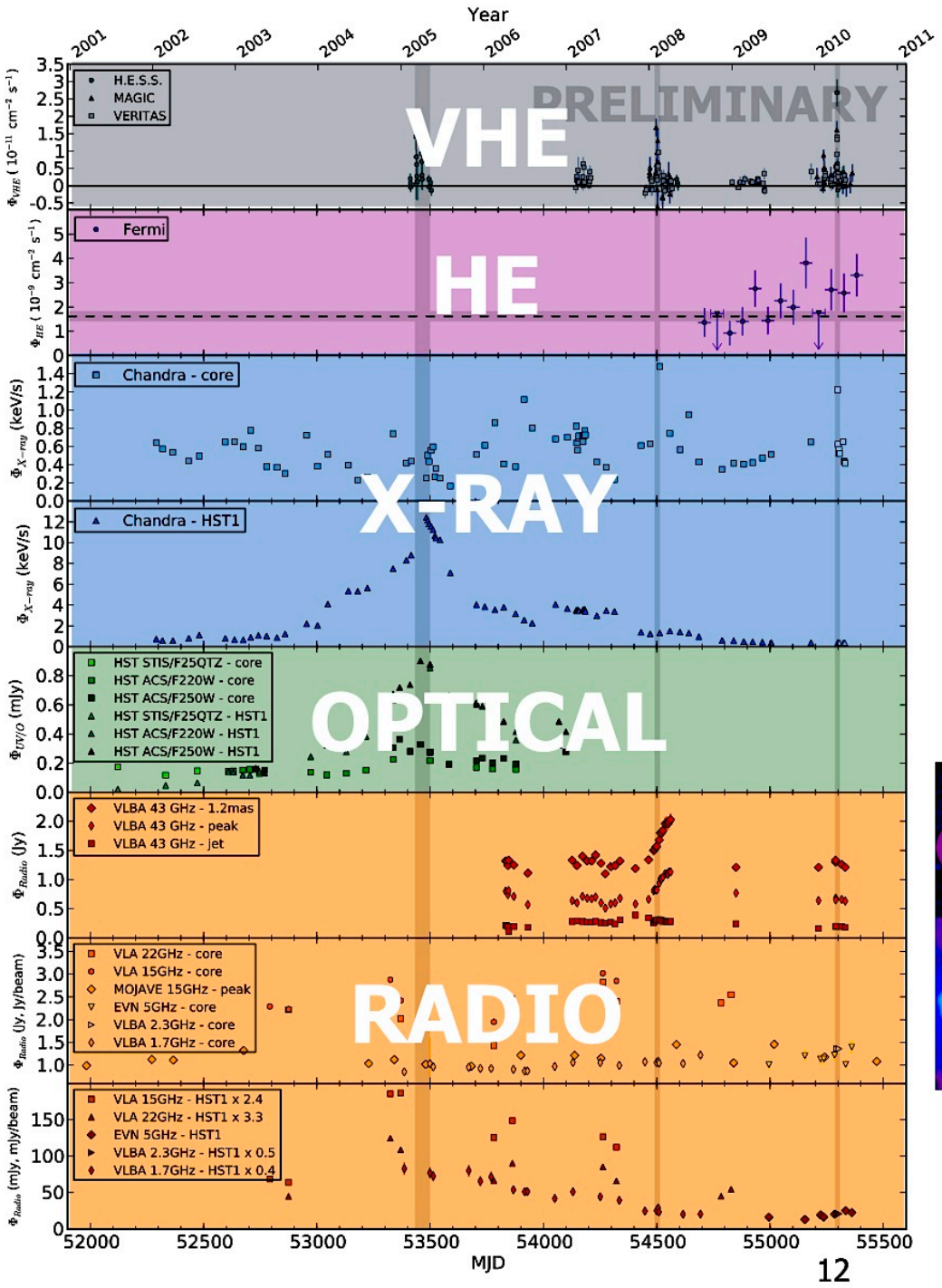

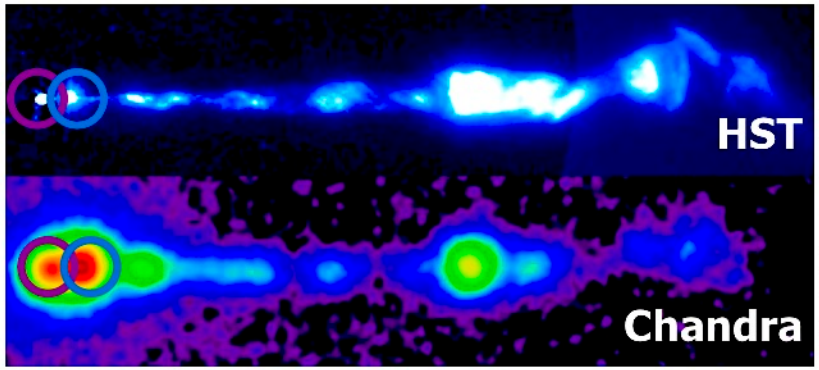

Madrid et al. 2007

Conclusions

Recent observations of blazar sources in X-rays (Suzaku, Swift) and gamma-rays (Fermi/LAT, HESS, Magic, VERITAS), together with massive MWL campaigns carried out during the last years, allowed us to address the some open questions regarding the physics of AGN and relativistic jets:

- **Internal structure of relativistic jets**
  Most of the energy in blazar sources is dissipated relatively far from the central engine, at the scales $>10^3$ R_g ~ 10^{17} cm. Rapid and rare high-energy flares may originate either extremely close to supermassive black holes, or further away, within extremely compact sub-volumes of the outflows.

- **Jet content and energetics**
  Around the blazar emission zone, AGN jets seem already matter-dominated. In addition, the total kinetic power of the outflows seems to be carried predominantly by cold, or at least mildly-relativistic protons (proton-to-electron number density ratio $N_{p+}/N_{e\pm}$ ~ 0.1). All the observed radiative output of blazars is however dominated by the synchrotron and inverse-Compton emission of ultrarelativistic electrons, and no radiative signatures of hadrons have been found.

- **Particle acceleration processes**
  Energy spectra of ultrarelativistic electrons dominating broad-band emission of blazar sources are well approximated by a multiply-broken power-law form, at least during the quiescence states. Such a form is hardly consistent with the predictions of the 1st order Fermi acceleration at non-relativistic shocks. On the other hand, the blazar electron spectra seem qualitatively consistent with the ones expected to form at relativistic, perpendicular and proton-mediated shocks. The alternative spectral shapes (ultrarelativistic Maxwellians, for example) are still allowed, though in principle not needed (with a possible exception of flaring states of BL Lacs, which are hardly explored and covered across the electromagnetic continuum, and which may involve “non-standard” particle spectra and alternative acceleration).

Buckup Slides

Large-scale Quasar Jets

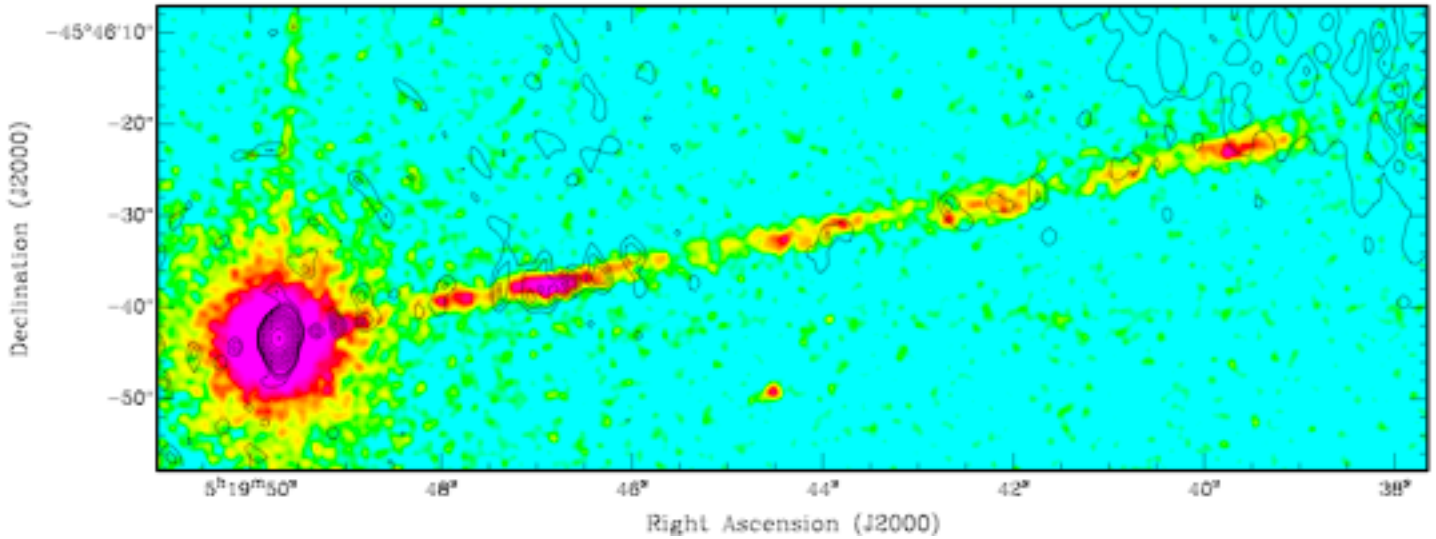

Marshallet al. 10

Chandra X-ray Observatory detected surprising variability of the knot in 100 kpc-scale jet of Pictor A (~4σ level).

At this distance from the core, we expect only >1000-yr-variability timescale; the observed X-ray variability timescale is however 1-10 yr. This suggest sub-structure of the outflow, and bulk of the observed emission produced in a tiny sub-volume of the jet.

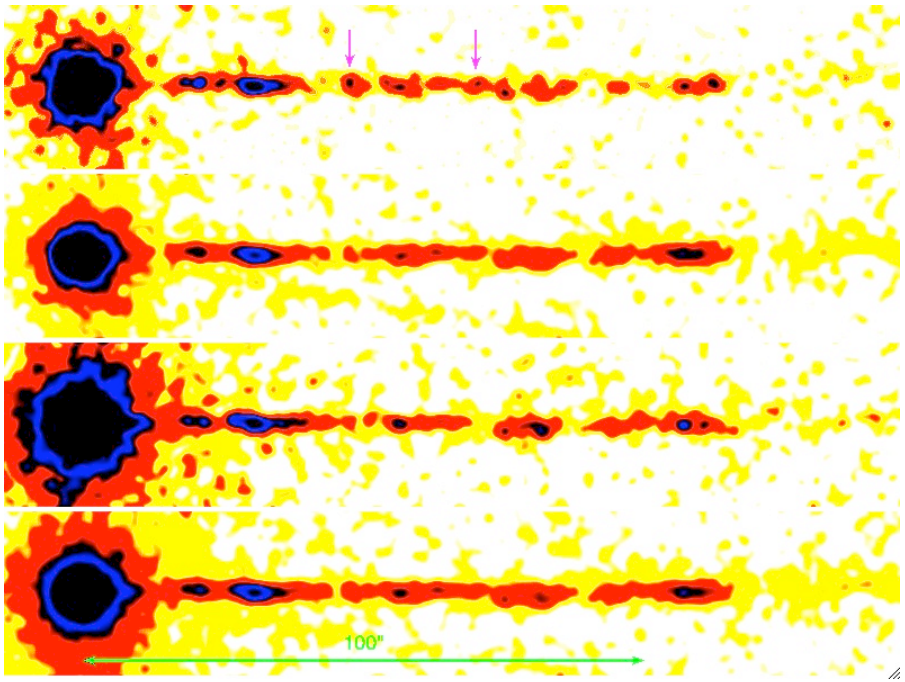

EBL-related Absorption

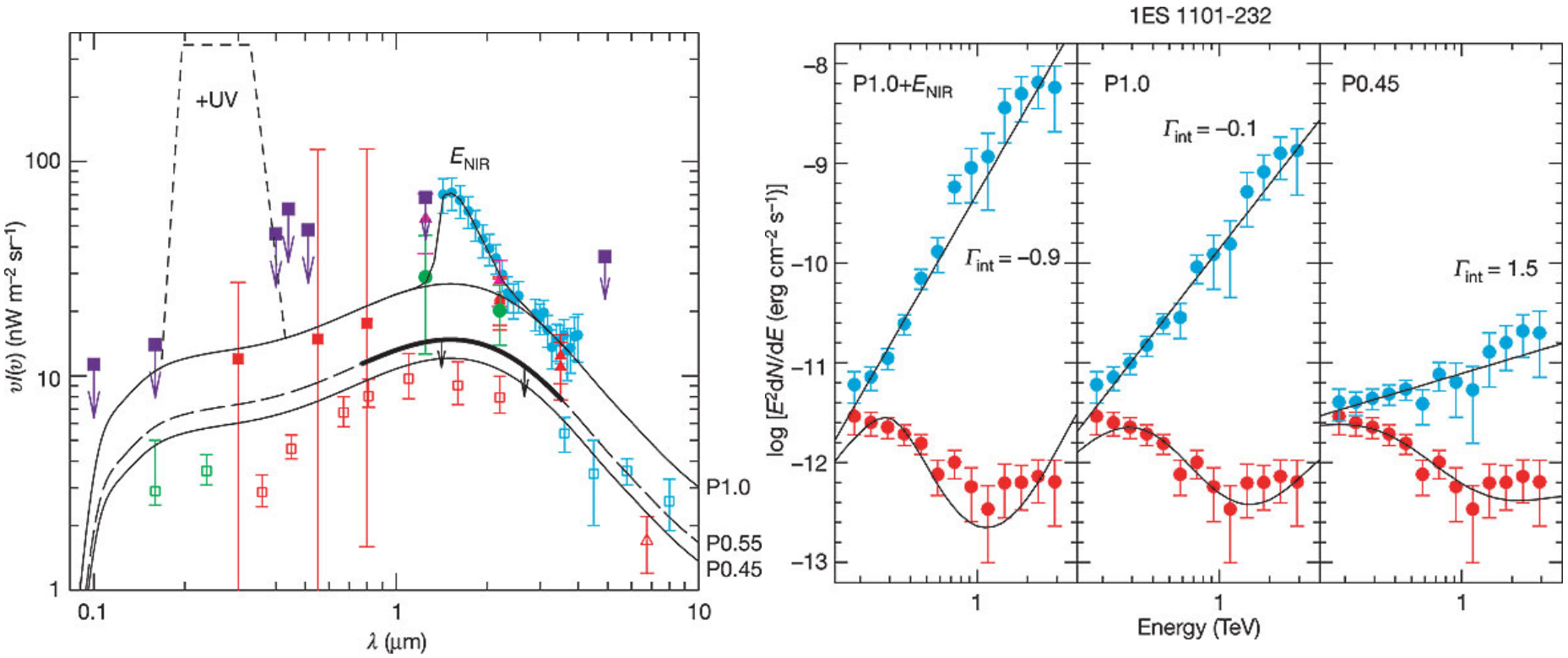

Aharonian et al. 06 [HESS]: The intrinsic gamma-ray spectrum of the distant blazar 1ES 1101-232 (z=0.186), when corrected for the EBL absorption effects, is very flat. In particular, assuming the level of EBL as claimed in Primack+01 and the NIR excess claimed by Matsumoto+05 ("P1.0+ENIR"), as well as a power-law form of the gamma-ray continuum $S(\nu) \propto \nu^{-\alpha}$, the intrinsic gamma-ray spectral index becomes $\alpha_{int} \equiv \Gamma_{int} - 1 = -1.9$. Only excluding the NIR excess and scaling the shape of the EBL as given by Primack+ 01 by a factor of 0.45, the intrinsic spectral index becomes $\alpha_{int} = +0.5$ (which is considered as a "reasonable one").

High Low-Energy Cut-off?

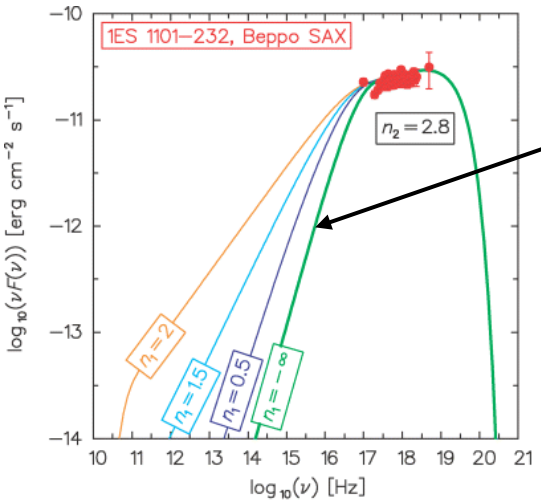

the flattest synchrotron spectrum
$\alpha = -1/3$

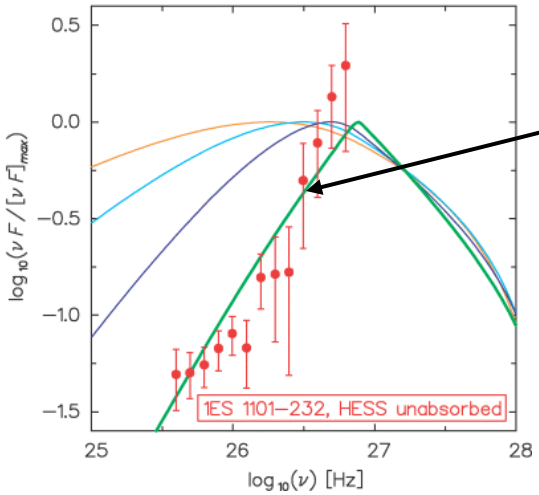

corresponding (Th. regime) SSC spectrum
$\alpha = -1/3$

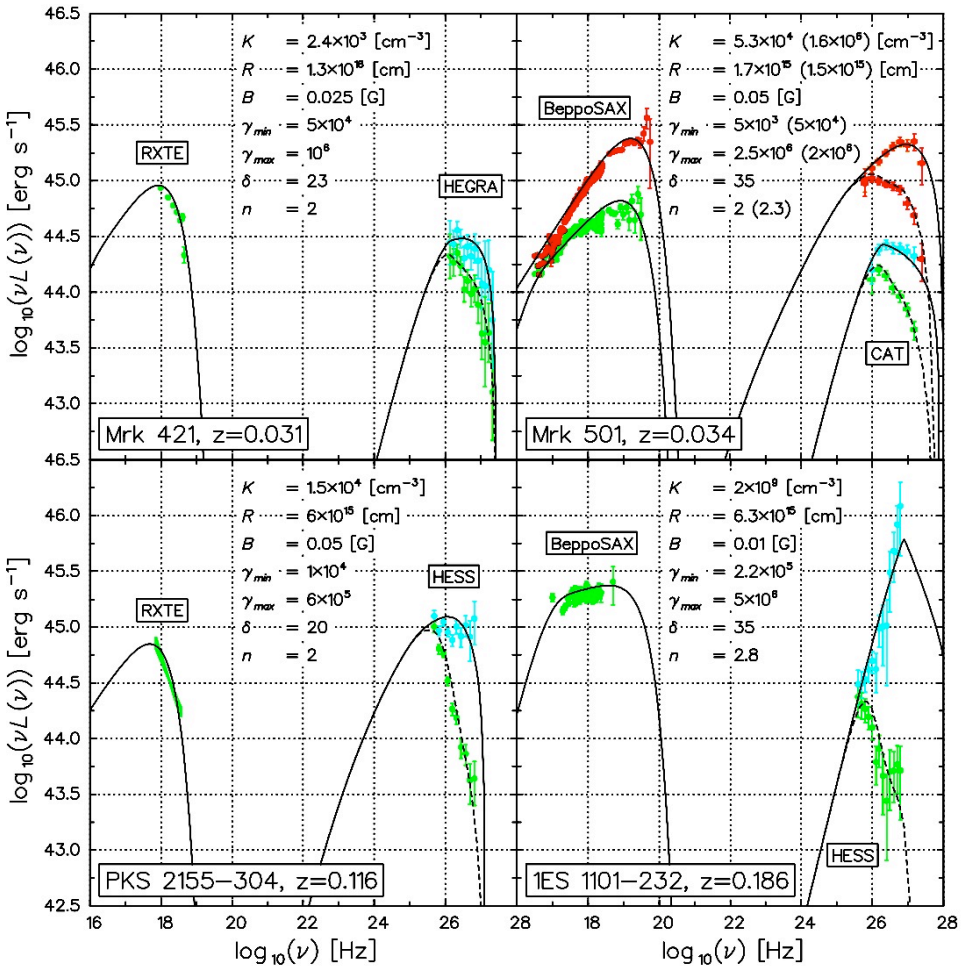

Katarzynski+ 06: Assuming very narrow-band electron energy distribution, between $\gamma_{min} \sim 10^5$ and $\gamma_{max} \sim 10^7$, it is possible (for some particular set of model free parameters) to fit the X-ray and TeV spectrum of 1ES 1101-232 with much higher level of the EBL.

Reconfinement Shocks

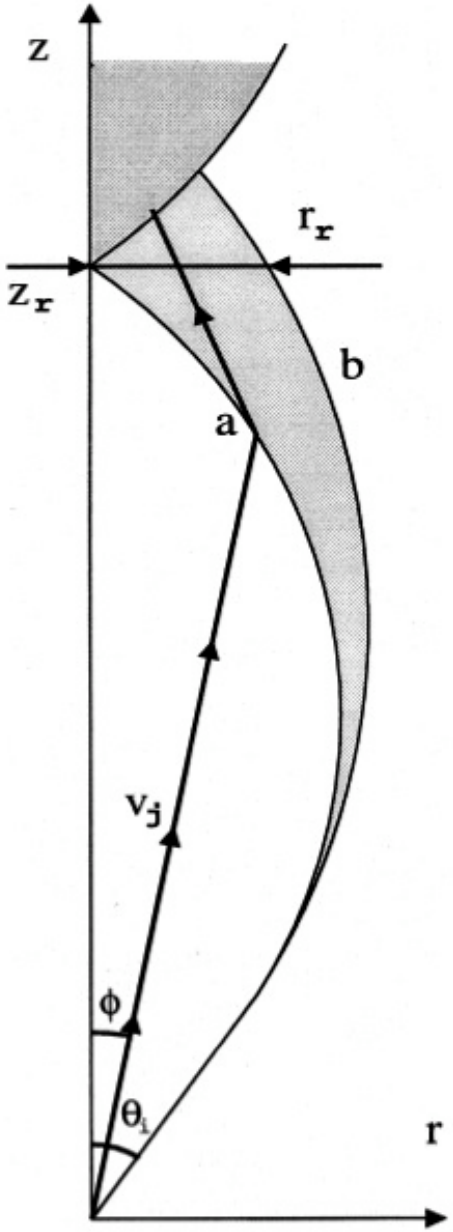

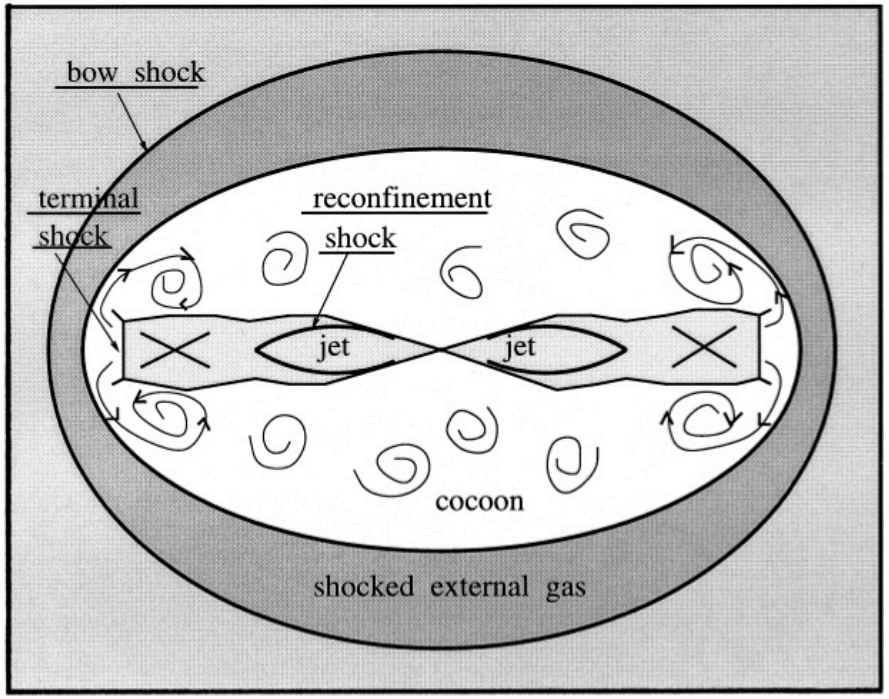

Stationary knots in astrophysical jets may be understood as nozzles of reconfinement shocks formed within supersonic outflows confined by their extended overpressured lobes, or by the ambient medium.

e.g., Sanders 83, Komissarov & Falle 97, Jorstad et al. 01, Stawarz et al. 06, Nalewajko & Sikora 09, Bromberg & Levinson 09.